Declaration

Honorable Commissioner of Patents:

I, Xu Youhao, hereby declare that:

1. I'm living in Beijing, People's Republic of China.

2. I'm a citizen of People's Republic of China.

3. From September 1981 to July 1985, I studied in the Department of Petroleum Refining in East China University of Science and Technology and obtained my Bachelor's degree; from September 1985 to July 1987, I studied in the Department of Chemical Engineering in East China University of Science and Technology and obtained my Master's degree; from September 2001 to December 2006, I studied in the Research Institute of Petroleum Processing and obtained my Doctor's degree.

4. Since August 1987, I've been devoting myself to the development of catalytic cracking technology in the Research Institute of Petroleum Processing, and have twenty years' experience. I took part in the development of Deep Catalytic Cracking (DCC) technology, and I'm currently in charge of the development and application of a newly series of FCC processes for producing maximum isoparaffins in cracked naphtha or clean gasoline and propylene (MIP and MIP-CGP). I have written more than forty papers on this subject, six of which were published in internationally significant periodicals and international academic conferences, and applied for, altogether, more than seventy patents domestically and abroad.

5. In US Patent Application 09/553,990, I propose a novel riser reactor, wherein the ratio of the diameter of a second reaction zone to the diameter of a first reaction zone ranges from 1.5: 1 to 5: 1. However, in catalytic cracking of the prior art, the ratio of the diameter of a second reaction zone to the diameter of a first reaction zone in a riser reactor should be less than 1.5: 1.

6. On the basis of the European patent EP0171460, Kmecak et al., the Examiner in charge of this application drew the conclusion, after manually

making a measurement in Figure 8 of EP0171460, that "DR_2: DR_1 is equal to approximately 3: 1". In my point of view, this is impossible because of the following reasons:

6.1. In catalytic cracking of the prior art, the ratio of the diameter of a so-called second reaction zone to the diameter of a so-called first reaction zone in a riser reactor should be less than 1.5: 1.

6.2. Figure 8 in EP0171460 is merely a schematic drawing without the specific dimensions available. Thus, the value obtained by manual measurement on the basis of the schematic drawing is inaccurate. One skilled in the art would never do this.

6.3. If "DR_2: DR_1 is equal to approximately 3: 1", it will be obtained upon scientific calculation (see Items 8 and 9 for details) that the ratio of the velocity at the outlet of the first reaction zone to the velocity at the inlet of the first reaction zone, i.e. u_1/u_0, is 18.7, which is far greater than the generally recognized ratio of less than 3 in the art. Thus, the Examiner's conclusion cannot be fulfilled.

7. In my point of view, the present invention achieves unexpected technical effects, which can be seen clearly from Example 1, Example 2, Example 3 and the corresponding Comparative Example, as given herein below.

The Comparative Example A and Example 3 are complementary tests. Example 1 and Example 2 are recited in the original application document. The properties of feedstock used in the Examples and the Comparative Example A and the properties of the catalyst are respectively listed in Tables 1 and 2.

Example 1

This Example showed the use of catalyst A in a novel pilot plant riser reactor according to the present invention for the production of isobutane and isoparaffin-enriched gasoline by means of catalytic conversion in the riser reactor.

The total height of the prelift zone, the first reaction zone, the second reaction zone, the outlet zone of the riser reactor was 15 meters, in which the

height of the prelift zone with the diameter of 0.025 meter was 1.5 meters, the height of the first reaction zone with a diameter of 0.025 meter was 4 meters, the height of the second reaction zone with a diameter of 0.1 meter was 6.5 meters, the height of the outlet zone with a diameter of 0.025 meter was 3 meters. The isotrapezia vertex angle of the vertical section of the conjunct section between the first reaction zone and the second reaction zone was 45°. The isotrapezia base angle of the vertical section of the conjunct section between the second reaction zone and the outlet zone was 60°.

The operating conditions and product slate are listed in Table 3, and the gasoline properties are listed in Table 4.

Example 2

This Example showed the use of gasoline with high olefin content as a quenching medium in a novel riser reactor for the production of isoparaffin enriched gasoline by means of catalytic conversion in the riser reactor.

The total height of the prelift zone, the first reaction zone, the second reaction zone, the outlet zone of the riser reactor was 15 meters, in which the height of the prelift zone with the diameter of 0.025 meter was 1.5 meters, the height of the first reaction zone with a diameter of 0.025 meter was 4 meters, the height of the second reaction zone with a diameter of 0.05 meter was 6.5 meters, the height of the outlet zone with a diameter of 0.025 meter was 3 meters. The isotrapezia vertex angle of the vertical section of the conjunct section between the first reaction zone and the second reaction zone was 45°. The isotrapezia base angle of the vertical section of the conjunct section between the second reaction zone and the outlet zone was 60°.

The catalyst and gasoline feedstock used in this Example were the same as those used in Example 1. The gasoline produced in comparative example 1 of the original description as a quenching medium was charged into the conjunct section between the first reaction zone and the second reaction zone. The other steps were basically the same as those in Example 1.

The operating conditions and product slate are listed in Table 3, and the gasoline properties are listed in Table 4.

Example 3

This Example showed the use of gasoline with high olefin content as a quenching medium in a novel pilot plant riser reactor according to the present invention for the production of isobutane and isoparaffin enriched gasoline by means of catalytic conversion in the riser reactor.

The total height of the prelift zone, the first reaction zone, the second reaction zone, the outlet zone of the riser reactor was 15 meters, in which the height of the prelift zone with the diameter of 0.025 meter was 1.5 meters, the height of the first reaction zone with a diameter of 0.025 meter was 4 meters, the height of the second reaction zone with a diameter of 0.0375 meter was 6.5 meters, the height of the outlet zone with a diameter of 0.025 meter was 3 meters. The isotrapezia vertex angle of the vertical section of the conjunct section between the first reaction zone and the second reaction zone was 45°. The isotrapezia base angle of the vertical section of the conjunct section between the second reaction zone and the outlet zone was 60°.

The catalyst and gasoline feedstock used in this Example were the same as those used in Example 1. The gasoline produced in comparative example 1 of the original description as a quenching medium was charged into the conjunct section between the first reaction zone and the second reaction zone. The other steps were basically the same as those in Example 1.

The operating conditions and product slate are listed in Table 3, and the gasoline properties are listed in Table 4.

Comparative Example A

Compared with the previous Example 2, this comparative example was conducted under the same condition except that the diameter of the second reaction zone is 0.03 meters and thus the diameter ratio of the second reaction zone to the first reaction zone is 1.2:1.

The operating conditions and product slate are listed in Table 3, and the gasoline properties are listed in Table 4.

It can be seen clearly from Tables 3 and 4 that:

1) In Example 1, 5.65wt% of LPG was isobutane;
In Example 2, 5.98wt% of LPG was isobutane;
In Example 3, 5.62wt% of LPG was isobutane;
however In Comparative Example, 3.02 wt% of LPG was isobutane (see Table 3);

2) In Example 1, Iso-paraffins in gasoline was 36.00wt%;
In Example 2, Iso-paraffins in gasoline was 43.86wt%;
In Example 3, Iso-paraffins in gasoline was 34.8wt%;
however In Comparative Example, Iso-paraffins in gasoline was 21.33wt%(see Table 4);

In other words, when the ratios of the diameter of the second reaction zone to the diameter of the first reaction zone are 4:1, 2:1 or 1.5:1 respectively, the present invention has a significant advantage in respect of effects over the prior art in which the corresponding diameter ratio is 1.2: 1.

Table 1

Density (20 °C), kg/m^3	890.5
Kinematic Viscosity (100 °C), mm^2/s	5.08
Carbon Residue, wt%	0.7
Pour Point, °C	40
Total Nitrogen, wt%	0.16
Sulfur, wt%	0.53
Carbon, wt%	85.00
Hydrogen, wt%	12.62
Heavy Metal Content, ppm	
Ni	0.16
V	0.15
Fe	—
Cu	—
Na	0.45
Distillation, °C	
IBP	278
10%	385
30%	442
50%	499
70%	—
90%	—
EP	—

Table 2

Catalyst Name	A
Trade Mark	ZCM-7
Chemical Composition, wt%	
Aluminum Oxide	46.4
Sodium Oxide	0.22
Ferric Oxide	0.32
Apparent Bulk Density, kg/m^3	690
Pore Volume, ml/g	0.38
Surface Area, m^2/g	164
Attrition Index, wt% hr^{-1}	—
Particle Size Distribution, wt%	
0~40 microns	4.8
40~80 microns	47.9
>80 microns	47.3

Table 3

	Example 1	Example 2	Example 3	Comparative Example A
the diameter ratio of the second reaction zone to the first second reaction zone	4:1	2:1	1.5:1	1.2:1
Operation condition:				
Reaction Temperature, °C				
The First Reaction Zone	545	545	545	545
The Second Reaction Zone	495	495	495	495
Reaction Time, sec	5.0	5.3	5.0	5.0
The First Reaction Zone	1.0	0.8	1.5	2.2
The Second Reaction Zone	3.5	3.9	3.0	2.3
The Outlet Zone	0.5	0.6	0.5	0.5
C/O Ratio	4.5	5.0	4.5	4.5
S/O Ratio	0.05	0.05	0.05	0.05
Product Slate, wt%				
Dry Gas	1.83	1.78	1.95	4.65
LPG	16.11	17.51	16.54	13.17
in which Isobutane	5.65	5.98	5.62	3.02
Gasoline	46.86	47.98	46.33	42.59
LCO	23.44	22.30	23.50	23.12
HCO	7.77	6.22	7.65	10.17
Coke	3.88	4.00	4.00	6.00
Loss	0.11	0.21	0.03	0.30

Table 4

	Example 1	Example 2	Example 3	Comparative Example A
the diameter ratio of the second reaction zone to the first second reaction zone	4:1	2:1	1.5:1	1.2:1
Density (20 °C), kg/m^3	743.6	745.3	742.6	748.2
Octane Number				
RON	90.0	90.1	90	90.5
MON	79.0	80.9	79	79.3
Induction Period, min	>1000	800.0	>1000	343
Existent Gum, mg/100ml	2.0	2.0	2.0	2.0
Sulfur, wt%	0.0095	0.01	0.009	0.016
Nitrogen, wt%	0.0028	0.003	0.003	0.004
Carbon, wt%	86.14	86.51	86.15	86.72
Hydrogen, wt%	13.72	13.42	13.73	13.19
Distillation, °C				
IBP	46	48	46	48
10 %	73	75	73	75
30 %	95	97	95	96
50 %	114	118	114	120
70 %	143	144	143	145
90 %	171	173	171	173
EP	202	203	202	200
Gasoline composition, wt%				
Paraffins	41.01	47.87	40.01	25.61
in which Iso-paraffins	36.00	43.86	34.8	21.33
Naphthenes	7.20	7.45	7.0	6.5
Olefins	28.11	20.51	28.56	40.69
Aromatics	23.68	24.17	24.43	27.20

8. Directed at the part of "Response to Arguments" on pages 10-16 in the Office Action on December 13, 2007, I deem

(1). The density in Fig. 4 of US3246960 is fundamentally different from the density in my previous Declaration. The density mentioned in my previous Declaration is the density of gas in the riser reactor and the objects mentioned during the calculation are all gas, while the density in Fig. 4 of US3246960 is the density of mixture of gas and solid in the riser reactor (see column 4, line 74; column 2, lines 9-11). There are three reasons listed one by one below.

The first reason:

column 4, lines 73-74 of US3246960 clearly states that "the density of a fluidized mixture", and column 2, lines 9-10 clearly states that "…the suspension has an average density…";

The second reason:

According to the definition of the mixture of gas and solid (Powder Technology 82, 1995, Page 271)

$$\rho_m = \rho_g \times \varepsilon + \rho_p \times (1-\varepsilon)$$

wherin ρ_m represents the density of the mixture of gas and solid, ρ_g represents the density of gas, ρ_p represents the density of solid catalyst, ε represents voidage. Further conversion of the above equation produces:

$$\rho_m = \rho_p - (\rho_p - \rho_g) \times \varepsilon$$

Because $\rho_g << \rho_p$, the equation above can be simplified as:

$$\rho_m \approx \rho_p \times (1-\varepsilon)$$

The density of catalytic particles is usually 1500 kg/m^3, the range of the voidage in the riser reactor is usually 0.80~0.98 (the above equations and data are all common knowledge of a person ordinarily skilled in the art), so the density ρ_m of the mixture of gas and solid is 30~300 kg/m^3, i.e. 1.87~18.73 lb./cu.ft., which is consistent with 3.6~27.3 lb./cu.ft. in the right table of Figure 4, which proves that the data in Figure 4 of US3246960 is the density of the mixture of gas and solid rather than the density of the gas

mentioned in the present invention.

The third reason:

Figure 3-3-11 on pages 128-130, *Fluidized Catalytic Cracking Technology* (by Lu Chunxi and Wang Zhu' an, see Annex A1 and its English translation Annex A2 of the present Declaration) tests the average density of the mixture of gas and solid in the riser under various operating conditions is 46.3~53 kg/m^3, i.e 2.89~3.31 lb./cu.ft., which is consistent with that of 1~6 lb./cu.ft. in column 2, line 11 of US3246960. Said data further proves that the data in Figure 4 is the density of the mixture of gas and solid rather than the density of the gas mentioned in the present invention.

Furthermore it can also be seen that the density of the gas (i.e. ρ_1 mentioned in my previous Declaration) is far less than the density in Figure 4 of US3246960 (3.6~27.3 lb./cu.ft) from the below calculation (2).1) (i.e. 0.156lb./cu.ft. <<3.6~27.3 lb./cu.ft.).

(2). The Examiner questions the correctness of $\rho_1 = \rho_2$ in my previous Declaration.

Here I evidences based on the data of Chemical Engineering Science 62 (2007), Page 1184—1198(see ANNEX B) that $\rho_1 = \rho_2$ is correct. Based on the Figure 4 on Page 1193, cross section 1 and cross section 2 are respectively taken to simulate the two cross sections of First Reaction Zone Outlet and Second Reaction Zone Inlet,

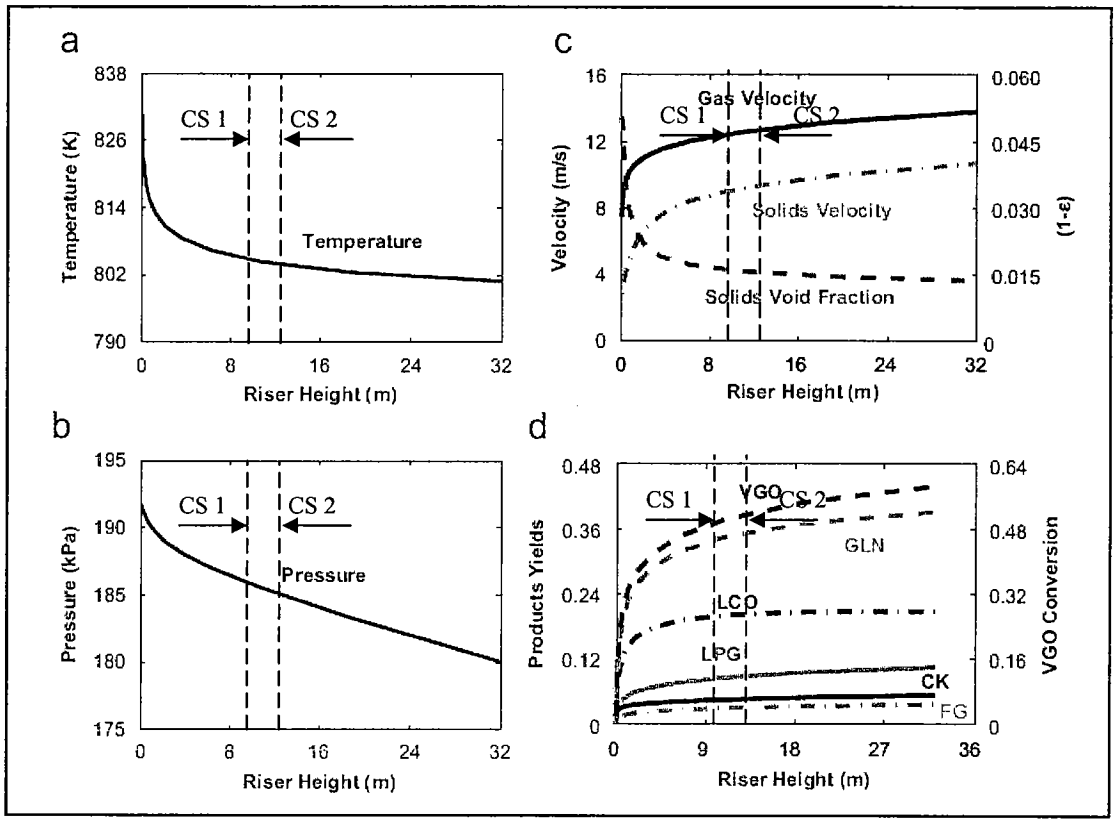

in which CS 1=cross section 1 and CS 2=cross section 2.

1) First Reaction Zone Outlet(cross section 1)

At the First Reaction Zone Outlet, Pressure P=185800Pa, Temperature T=532℃, and the gas is composed of:

Gas Components	Mass Fraction, wt%	Molar Mass, kg/kmol
Steam	5.89	18
Fuel Gas (FG)	2.79	20
Liquefied Petroleum Gas (LPG)	7.86	50
Gasoline (GLN)	33.27	100
LCO	18.41	200
Feedstock	31.78	500

The molar mass of the gas at this position can be calculated as

$$\frac{100}{5.89/18+2.79/20+7.86/50+33.27/100+18.41/200+31.78/500} = 89.9 \text{ kg/kmol}$$

and the density of the gas is

$$\frac{185800\times 89.9}{8.314\times(273+532)\times 1000} = 2.496 \text{ kg/m}^3 = 0.156 \text{ lb./cu. ft.}$$

2) Second Reaction Zone Inlet（cross section 2）

At the Second Reaction Zone Inlet, Pressure P=184714Pa，Temperature T=530℃，and the gas is composed of:

Gas Components	Mass Fraction, wt%	Molar Mass, kg/kmol
Steam	5.89	18
Dry Gas	3.23	20
Liquefied Gas	8.77	50
Gasoline	34.91	100
Diesel Fuel	19.64	200
Feedstock Oil	27.56	500

The molar mass of the gas at this position can be calculated as

$$\frac{100}{5.89/18+3.23/20+8.77/50+34.91/100+19.64/200+27.56/500} = 85.7 \text{ kg/kmol}$$

and the density of the gas is

$$\frac{184714\times 85.7}{8.314\times(273+530)\times 1000} = 2.37 \text{ kg/m}^3 = 0.148 \text{ lb./cu. ft.}$$

It is clear that the density of gas at cross section 1 ($\rho 1$) is 0.156 lb./cu.ft which is approximately equivalent to the density of gas at cross section 2 ($\rho 2$) of 0.148 lb./cu.ft. Thus it can be deemed that $\rho 1=\rho 2$.

(3). Page 12, Lines 10-14 of this Office Action states that "..... Furthermore, the disclosure of Kmecak, in combination with the teachings of Williams, would have suggested to one having ordinary skill in the art that the dimensions of the zones in the riser could be varied in order to optimize the reaction conditions, e.g., residence time, within a particular zone, for establishing the conversion of a particular hydrocarbon containing feed stream to the desired products."

I can not agree with the examiner. I deem that the adjustments to the diameter and length of riser （EP 0171460, Kmecak） are very limited other

than unlimited.

According to the requirement of production, the structural dimensions of riser reactor (including diameter and length) are adjustable in design so as to obtain the best product distribution. But since catalytic cracking adopts catalysts containing zeolite molecular sieve, and the reactions are very quick, the riser reactors used in the current industry imposes stringent requirements on the reaction time, which is usually 2-3 seconds. Therefore, the adjustments to the diameter and length of riser are very limited other than unlimited. For example,

1) Regarding the riser with the length of 49m and the diameter of 1.2m, if the reaction time is 2 seconds, the volume flow is:

$$\frac{49}{2}\times\pi\times\frac{1.2^2}{4}=27.7088\ m^3/s$$

If the reaction time is changed to 3 seconds, then when the volume flow and the length of the riser are the same, the diameter of the riser is:

$$\sqrt{\frac{27.7088\times4\times3}{49\times\pi}}=1.47\ \text{m}$$

Thus, it can be seen that when other conditions do not change, and the reaction time is extended from 2 seconds to 3 seconds, the diameter of the riser is increased from 1.2m to 1.47m, the range of increase being very limited and the ratio of the two being merely 1.225:1.

2) If the diameter of the riser does not change (1.2m), then when the reaction time is extended from 2 seconds to 3 seconds, under the condition of the same processing quantity, the height of the riser will increase from 49m to 73.5m, which is usually not adopted in engineering due to very high investment and operating cost.

It can be seen from the above example that conventional FCC riser reactors are restricted by reaction time and thus the range of its diameter change is very limited in engineering designs, the expansion ratio of the diameters usually being less than 1.5:1. The present invention starts with catalytic cracking reaction chemistry and breaks through the intrinsic concept mainly based on cracking in conventional FCC reactions. Cracking reactions and conversion reactions are conducted respectively in different reaction zones, thereby extremely extending the reaction time of catalytic

cracking reactions up to 3-25 seconds, such that the expansion ratio of the diameters in different reaction zones can reach 1.5 :1~5.0:1.

(4). Here I detailedly prove that the diameter ratio of the second reaction zone to the first reaction zone does not exceed 1.5:1, to say nothing of 3.0:1 in the reference EP 0171460(Kmecak) as cited by the Examiner by referring to Fig 1.

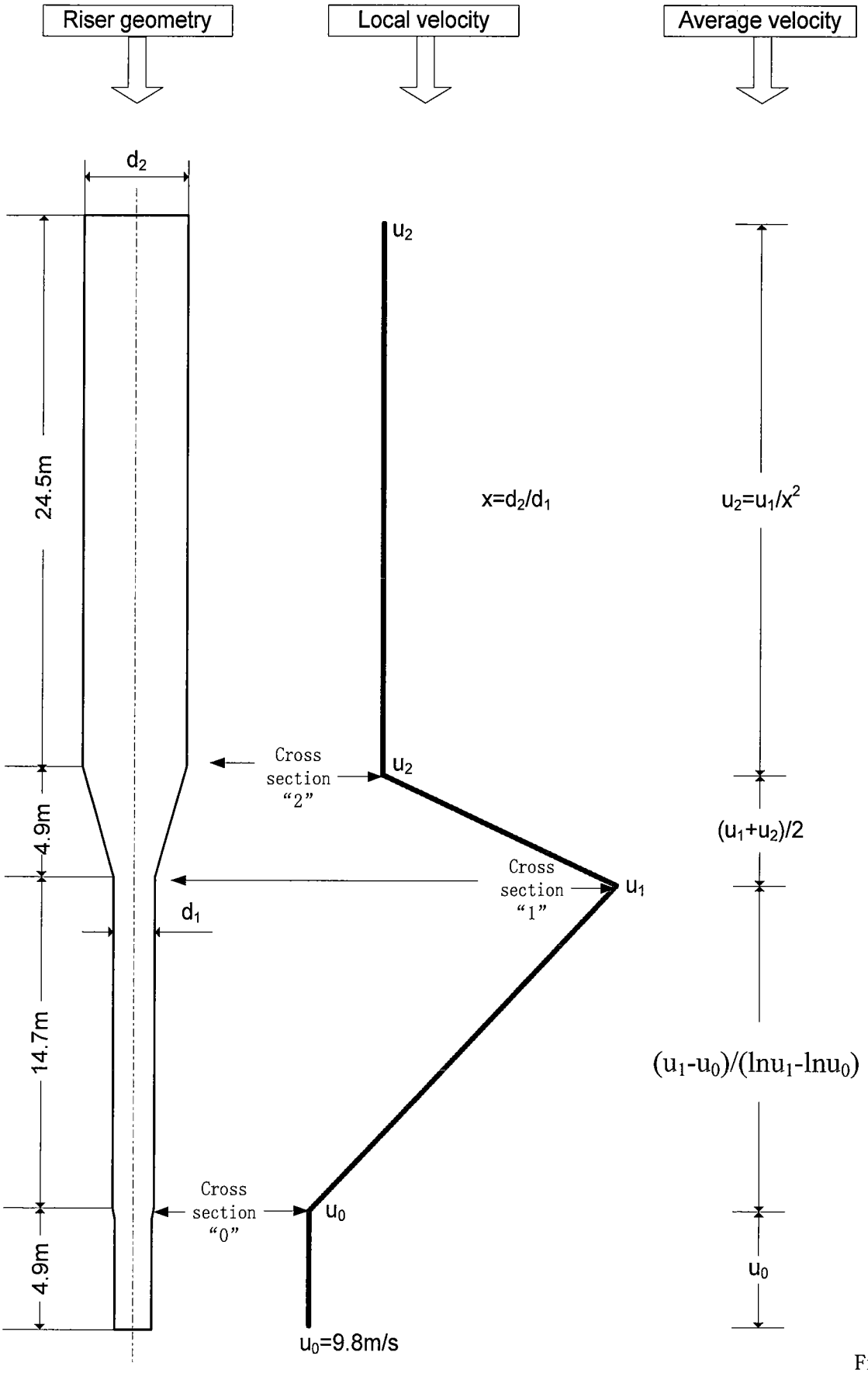
Riser geometry
Local velocity
Average velocity
d2
u2
24.5m
x=d2/d1
u2=u1/x2
Cross section "2"
u2
4.9m
(u1+u2)/2
Cross section "1"
u1
d1
14.7m
(u1-u0)/(lnu1-lnu0)
Cross section "0"
u0
4.9m
u0
u0=9.8m/s

Fig. 1

1). The symbols are defined as follows:
u—velocity, m/s;
h—height of the riser, m
t—residence time, s
V—volume flow rate, m^3/s;
A—cross-sectional area of the riser, m^2;
d—diameter of the riser, m;
x—ratio of the diameter of the second reaction zone to the diameter of the first reaction zone, dimensionless;
P—pressure, Pa;
M—molar mass, g/mol;
R—gas constant, 8.314 J/mol•K;
T—temperature, K
ρ—density, kg/m^3.

2). Symbols t, ρ and V are defined by the following equations:

$$t = \frac{h}{u} \quad (1)$$

$$\rho = \frac{P \times M}{R \times T} \quad (2)$$

$$V = u \times A = u \times \pi \times \left(\frac{d}{2}\right)^2 \quad (3)$$

3). Prerequisites or Assumptions for said Deduction

I. No chemical reaction occurs in the prelift zone, the fluid is in a uniform motion state, and the average velocity is represented by u_0.

II. The velocity in the first reaction zone exhibits a logarithmic increase tendency along the axial direction of the riser, and the average velocity in the first reaction zone is represented by the logarithmic mean value of the velocity at the inlet (u_0) and the velocity at the outlet (u_1), which is calculated as described hereinbelow:

$$\frac{u_1 - u_0}{\ln u_1 - \ln u_0}$$

III. The basic reactions in the second reaction zone are conversion

reactions, and molecular expansion may be neglected. The state of the fluid may approximately be regarded as uniform motion state. The average velocity is presented by u_2.

IV. The velocity in the conjunct section between the first and second reaction zones exhibits a linear decrease tendency along the axial height of the riser, and the average velocity is presented by the mean value of the velocity at the inlet (u_1) and the velocity at the outlet (u_2), which is calculated as described hereinbelow:

$$\frac{u_1 + u_2}{2}$$

4). Detailed Deduction Procedure:

Based on the above-mentioned prerequisites or assumptions for deduction and the data disclosed in EP0171460 (the height of the prelift zone is 4.9 m, the height of the first reaction zone is 14.7 m, the height of the conjunct section between the first and second reaction zone is 4.9 m, the height of the second reaction zone is 24.5 m, the total height of the riser is 49 m and the average velocity in the whole riser is 24.5 m/s), the residence time in the whole riser is calculated as described hereinbelow:

$$\frac{4.9\text{m}}{u_0} + \frac{14.7\text{m}}{\frac{u_1 - u_0}{\ln u_1 - \ln u_0}} + \frac{4.9\text{m}}{\frac{u_1 + u_2}{2}} + \frac{24.5\text{m}}{u_2} = \frac{49\text{m}}{24.5\text{m/s}} \qquad (4)$$

It can be seen from the data provided by the Examiner that u_0=9.8 m/s, and thus Equation (4) may be written as:

$$\frac{4.9\text{m}}{9.8\text{m/s}} + \frac{14.7\text{m}}{\frac{u_1 - 9.8\text{m/s}}{\ln u_1 - \ln 9.8\text{m/s}}} + \frac{4.9\text{m}}{\frac{u_1 + u_2}{2}} + \frac{24.5\text{m}}{u_2} = 2\text{s} \qquad (5)$$

According to the law of conservation of mass, the mass flowrates at all cross-sections of the riser are equal, and, in terms of Figure 1, the mass flowrate at the inlet of the conjunct section between the first and second reaction zones (shown by the subscript "1") and the mass flowrate at the outlet of the conjunct section between the first and second reaction zones (shown by the subscript "2") are equal, as shown by the following equation:

$$\rho_2 \times V_2 = \rho_1 \times V_1 \qquad (6)$$

The general knowledge of the principles of catalytic cracking teaches us that the reactions occurring at cross-section "1" and cross-section "2" are basically conversion reactions and cracking does not occur in a large scale. Accordingly, it may be concluded that the number of molecules at said two cross-sections remains unchanged. Since the pressures and temperatures at said two cross-sections do not change much, it may be concluded, on the basis of the density definition, i.e. equation (2), that the densities at said two cross-sections are equal:

$$\rho_2 = \rho_1 \qquad (7)$$

Equation (6) can thus be written as:

$$V_2 = V_1 \qquad (8)$$

Upon substitution of the mass flowrate definition, i.e. Equation (3), into Equation (8), a new equation is obtained, which is as follows:

$$u_2 \times \pi \times \left(\frac{d_2}{2}\right)^2 = u_1 \times \pi \times \left(\frac{d_1}{2}\right)^2 \qquad (9)$$

Equation (9) is transformed to obtain the following equation:

$$u_2 = \frac{u_1}{\left(\frac{d_2}{d_1}\right)^2} = \frac{u_1}{(x)^2} \qquad (10)$$

The following monadic nonlinear equation about u_1 is thus obtained by substituting Equation (10) into Equation (5):

$$0.5s + \frac{14.7m}{\frac{u_1 - 9.8m/s}{\ln u_1 - \ln 9.8m/s}} + \frac{4.9m}{\frac{u_1 + \frac{u_1}{x^2}}{2}} + \frac{24.5m}{\frac{u_1}{x^2}} = 2s \qquad (11)$$

The Examiner believes that the ratio of the diameter of the second reaction zone to the diameter of the first reaction zone is 3, which means that x=3 in Equation (11). The following result is then obtained by solving Equation (11):

$$u_1 = 183.3\text{m/s} \quad (13)$$

Obviously,

$$\frac{u_1}{u_0} = \frac{183.3\text{m/s}}{9.8\text{m/s}} = 18.7 \quad (14)$$

The ratio of 18.7 is far greater than the generally recognizable ratio of less than 3 in the art.

Even when the ratio of the diameter of the second office zone to the first office action is 1.5:1, i.e. x=1.5, The following result is then obtained by solving Equation (11):

$u_1 = 62.8$ m/s

Obviously

$$\frac{u_1}{u_0} = \frac{62.8}{9.8} = 6.4$$

This value is even greater than 3.

Thus, the Examiner's opinion that "DR_2: DR_1 is equal to approximately 3: 1" is incorrect and impossible.

5) To further demonstrate that u_1/u_0<3, please see the following deduction based on prior art.

Deduction 1:

According to the law of conservation of mass, the mass flowrate at the inlet of the first reaction zone (corresponding to cross section "0" in Figure 1) and the mass flowrate at the outlet of the first reaction zone (corresponding to cross section "1" in Figure 1) are equal, i.e.

$$\rho_1 \times V_1 = \rho_0 \times V_0 \quad (15)$$

The definition of density (equation (2)) and the definition of the volume flow (equation (3)) are substituted into equation (15), and it produce:

$$\frac{P_1 \times M_1}{R \times T_1} \times u_1 \times A = \frac{P_0 \times M_0}{R \times T_0} \times u_0 \times A \qquad (16)$$

Transform equation (16) and produce:

$$\frac{u_1}{u_0} = \left(\frac{P_0}{P_1}\right) \times \left(\frac{T_1}{T_0}\right) \times \left(\frac{M_0}{M_1}\right) \qquad (17)$$

According to the general knowledge of the principles of catalytic cracking, one skilled in the art knows that the range of variation of pressure at the inlet and outlet of the first reaction zone is narrower than that of temperature, *i.e.* in equation (17):

$$\left(\frac{P_0}{P_1}\right) \times \left(\frac{T_1}{T_0}\right) < 1 \qquad (18)$$

Considering equation (18) in equation (17), it is easy to see that:

$$\frac{u_1}{u_0} < \frac{M_0}{M_1} \qquad (19)$$

Since reactions basically including cracking occur at the bottom of the riser (the so-called first reaction zone) after large-molecular feedstock oil contacts with a hot regenerated catalyst, the conversion of the feedstock in said zone increases rapidly, and a large amount of small-molecular products are produced, which is the manifestation of molecular expansion. It can be known that according to the typical distribution of catalytic cracking products, the ratio of the molar mass at the inlet and the outlet of the first reaction zone in the equation (19) is usually less than 3. The patent Examiner can find out that the distribution of many catalytic cracking products produces this ratio by calculation. Hereinbelow is a specific example for the Examiner's reference in the calculation of this ratio.

The calculation process of the gas composition and the molar mass thereof at the inlet of the first reaction zone is:

	Feedstock Oil Gas	Atomized Vapour
Mass Composition, wt%	90	10
Molar Mass, g/mol	500	18
Mol	$\frac{90g}{500g/mol}$	$\frac{10g}{18g/mol}$
Total Mol	$\frac{90g}{500g/mol}+\frac{10g}{18g/mol}$	
Molar Mass of the Mixed Gas, g/mol	$\frac{100g}{\frac{90g}{500g/mol}+\frac{10g}{18g/mol}}=135.95g/mol$	

The calculation process of the gas composition and the molar mass thereof at the outlet of the first reaction zone is:

	Dry Gas	Liquefied Gas	Gasoline	Diesel Fuel	Cycle Stock and Slurry Oil	Atomized Vapour
Mass Composition, w%	2.7	18	36	18	15.3	10
Molar Mass, g/mol	20	50	100	200	500	18
Mol	$\frac{2.7g}{20g/mol}$	$\frac{18g}{50g/mol}$	$\frac{36g}{100g/mol}$	$\frac{18g}{200g/mol}$	$\frac{15.3g}{500g/mol}$	$\frac{10g}{18g/mol}$
Total Mol	$\frac{2.7g}{20g/mol}+\frac{18g}{50g/mol}+\frac{36g}{100g/mol}+\frac{18g}{200g/mol}+\frac{15.3g}{500g/mol}+\frac{10g}{18g/mol}$					
Molar Mass of the Mixed Gas, g/mol	$\frac{100g}{\frac{2.7g}{20g/mol}+\frac{18g}{50g/mol}+\frac{36g}{100g/mol}+\frac{18g}{200g/mol}+\frac{15.3g}{500g/mol}+\frac{10g}{18g/mol}}=65.31g/mol$					

Thus, the ratio of the molar mass of the mixed gas at the inlet of the first reaction zone and at the outlet of the first reaction zone is:

$$\frac{M_0}{M_1}=\frac{135.95g/mol}{65.31g/mol}=2.08$$

i.e. in equation (19)

$$\frac{u_1}{u_0} < \frac{M_0}{M_1} = 2.08$$

Deduction 2:

I have provided three known references in my previous Declaration. They also prove my above viewpoint.

1) Figure 2 which illustrates the distribution of conversion along the axial direction of the height of the riser (In-Su Han, Chang-Bock Chung, *Chemical Engineering Science 56*, 2001, page 1954, see Annex I in my previous Declaration).

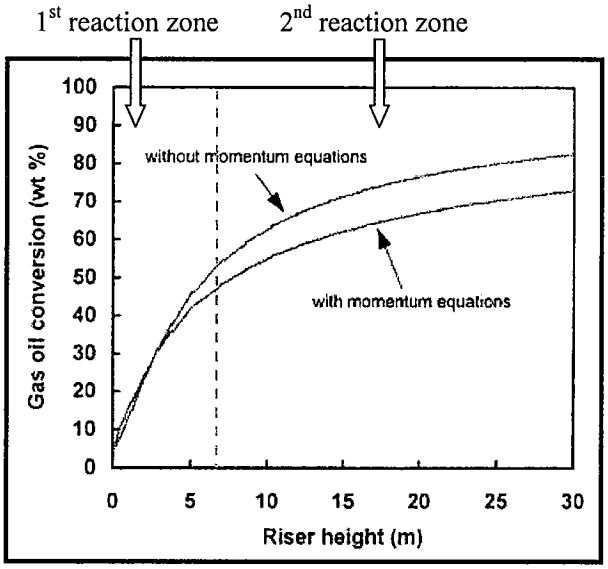

Fig 2: Distribution of conversion along the axial direction of the height of the riser

It is generally accepted in the art that the ratio of the velocity at the outlet of an iso-diameter riser(i.e. the so-called first reaction zone) to the velocity at the inlet of the iso-diameter riser(i.e. the so-called first reaction zone) is less than 3. This is exemplified by the following two examples:

First Example: Figure 3 illustrates the distribution of velocity along the axial direction of the height of the riser (In-Su Han, Chang-Bock Chung, *Chemical Engineering Science 56*, 2001, page 1978, see Annex II in my previous Declaration). It can be seen that the ratio of the velocity at the outlet of the first reaction zone to the velocity at the inlet of the first reaction zone (i.e. u_1/u_0 in Figure 2) is less than 2.

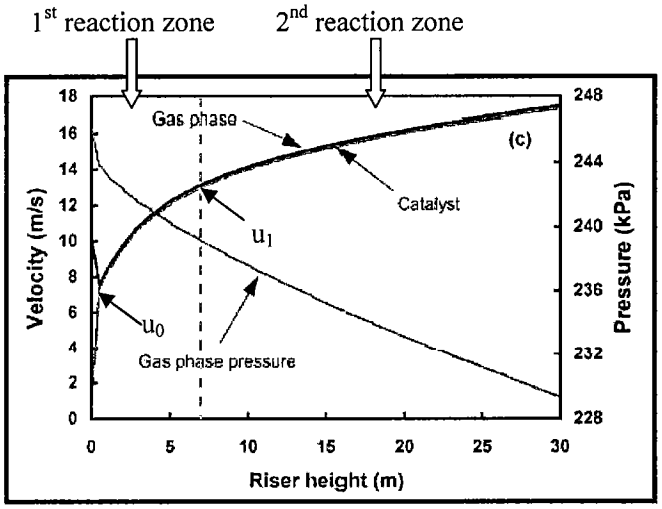

Fig. 3 Distribution of velocity along the height of the riser

Second Example: It can be readily seen from the reference *Process Calculation and Technical Analysis of Catalytic Cracking* (written by Cao Hanchang, Hao Xiren and Zhang Han, see Annex III, and the translation thereof, Annex IV in my previous Declaration), for example, the calculation results on page 242 (see also pages 5 and 6 of Annex IV) show a velocity of 11.45 m/s at the outlet of the riser, a velocity of 5.78 m/s at the inlet of the riser and a ratio of the former to the latter of 1.98.

9. Conclusions:

(1). The drawing in the reference （EP0171460, Kmecak et al）cited by the Examiner is a schematic drawing. An actual size can not be derived form this drawing.

(2). The velocity inside the riser of 18~31m/s or the residence time of 2s, mentioned by Kmecak et al , is much contradictory to the Examiner's opinion that the ratio of the diameter of the second reaction zone to that of the first reaction zone is 3, even 1.5. I respectfully deem that the Examiner's comments are incorrect.

10. I further declare that all statements made herein on personal knowledge are true and that all statements made on information and belief are believed to be true; and that these statements are made with the knowledge that willfully or intentionally false statements made by declaration to the United States Patent and Trademark Office are punishable by fine or imprisonment, or both, under 18

U.S.C. §1001; and that such willfully or intentionally false statements may jeopardize the validity and/or enforceability of the patent application with Appl. No. 09/553,990 and any United States Patent issuing therefrom.

Signed at Beijing this 10th day of March, 2008.

Xu Youhao

Dr. Xu Youhao

ANNEX A1

催化裂化流态化技术

卢春喜 王祝安 著

中国石化出版社

内 容 提 要

本书共分六章：流态化基本原理、气体分布器、工业催化装置的测试、新型催化裂化装置与若干新技术、催化裂化部分经验数据经验公式、催化裂化催化剂在管线中的流动。在叙述基本原理的基础上，着重结合设计与生产中的实际问题讲解，并介绍国内外发展的动态，供有关人员参考。

读者对象：从事催化裂化研究、设计与生产的工程技术人员，并可作为高校相关专业的研究生和本科生教材，也可供其他从事气固流化工作的人员参考。

图书在版编目(CIP)数据

催化裂化流态化技术/卢春喜，王祝安著.
—北京：中国石化出版社，2002
ISBN 7-80164-291-0

Ⅰ.催… Ⅱ.①卢…②王… Ⅲ.石油炼制-流化催化裂化
Ⅳ.TE624.4

中国版本图书馆 CIP 数据核字(2002)第 080378 号

中国石化出版社出版发行
地址：北京市东城区安定门外大街 58 号
邮编：100011 电话：(010)84271850
http://www.sinopec-press.com
E-mail:press@sinopec.com.cn
北京精美实华图文制作中心排版
北京金明盛印刷服务有限公司印刷
新华书店北京发行所经销
*
787×1092 毫米 16 开本 17 印张 429 千字
2002 年 11 月第 1 版 2004 年 11 月第 1 版第 2 次印刷
定价：35.00 元

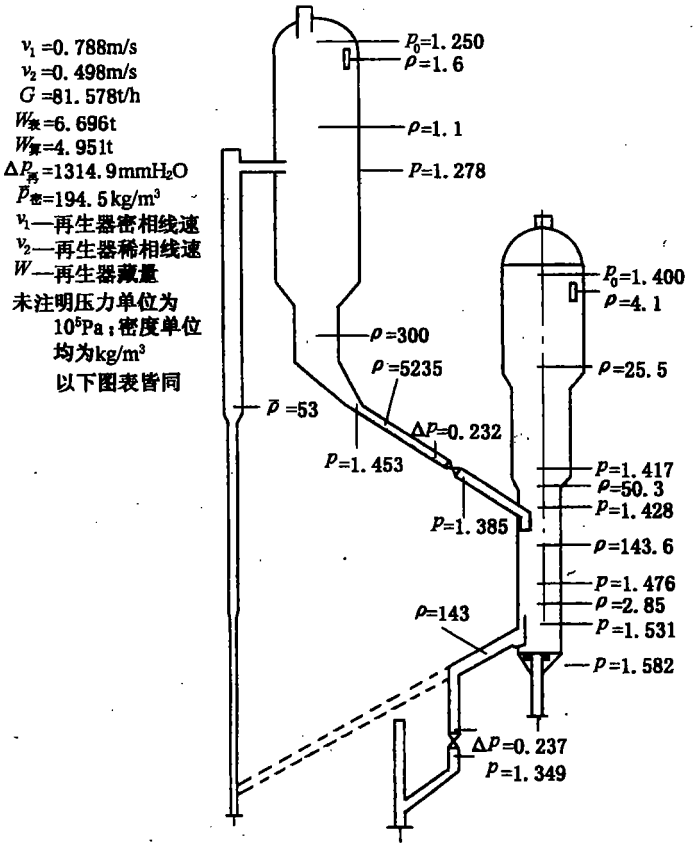

图 3－3－11(a)　系统各点压力及密度分布

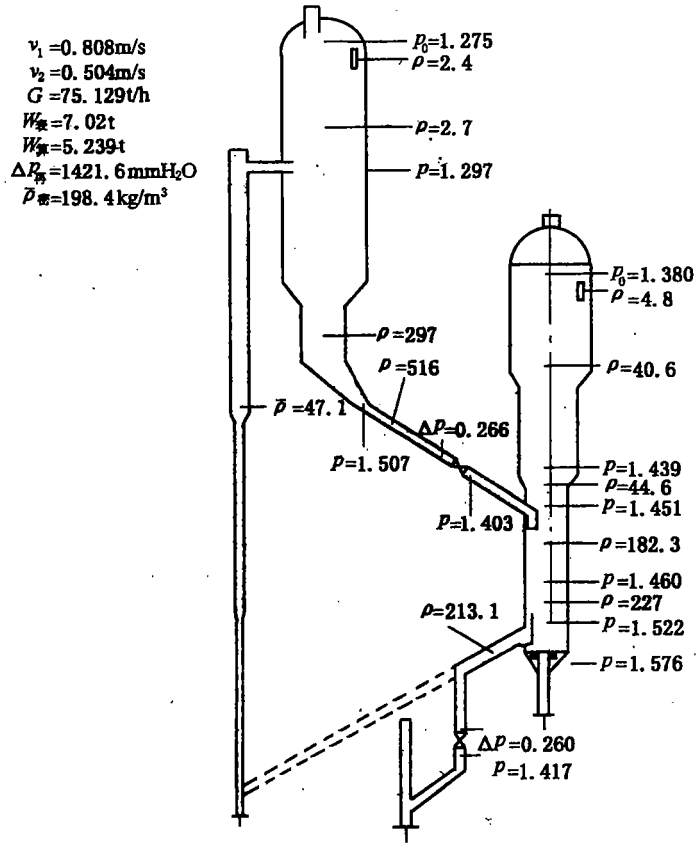

图 3－3－11(b)　系统各点压力及密度分布

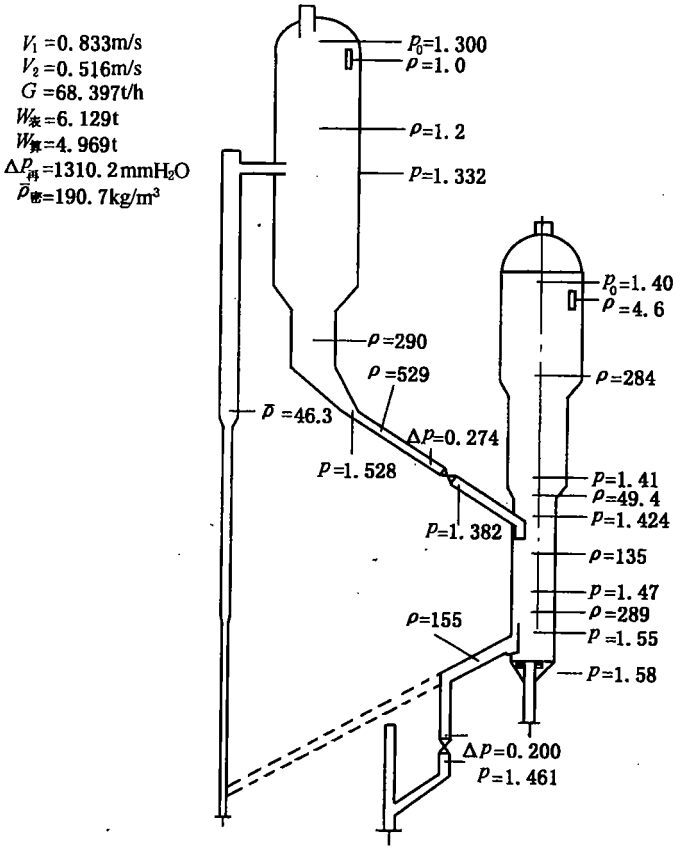

图 3-3-11(c)　系统各点压力及密度分布

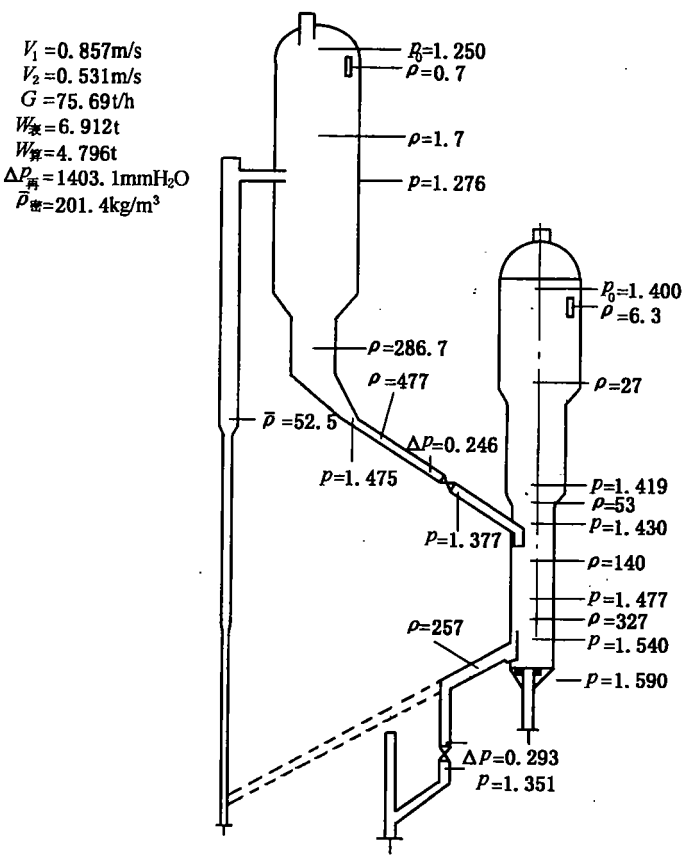

图 3-3-11(d)　系统各点压力及密度分布

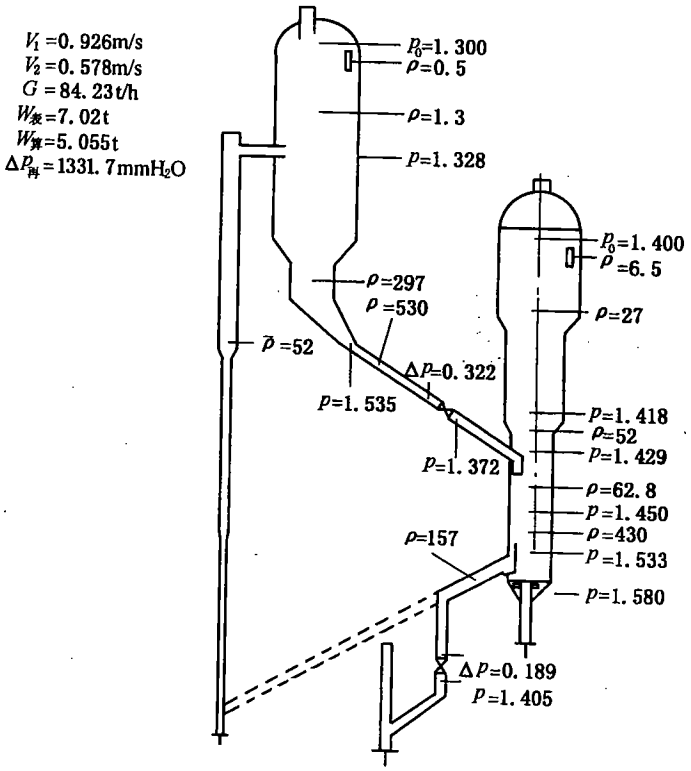

图 3-3-11(e) 系统各点压力及密度分布

3.2.3 再生器的催化剂密度分布规律

通过测试所得实际数据，经数据处理，标绘出沿再生器轴向催化剂密度分布曲线，见图 3-3-12。

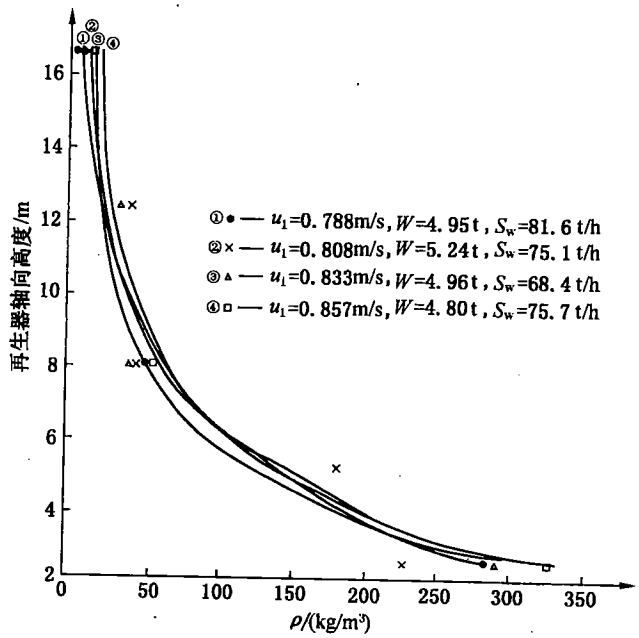

图 3-3-12 再生器密度分布曲线

FPCH00160004US

ANNEX A2

Fluidized Catalytic Cracking Technology

by Lu Chunxi and Wang Zhu'an

China Petrochemcal Press

内 容 提 要

本书共分六章:流态化基本原理、气体分布器、工业催化装置的测试、新型催化裂化装置与若干新技术、催化裂化部分经验数据经验公式、催化裂化催化剂在管线中的流动。在叙述基本原理的基础上,着重结合设计与生产中的实际问题讲解,并介绍国内外发展的动态,供有关人员参考。

读者对象:从事催化裂化研究、设计与生产的工程技术人员,并可作为高校相关专业的研究生和本科生教材,也可供其他从事气固流化工作的人员参考。

图书在版编目(CIP)数据

催化裂化流态化技术/卢春喜,王祝安著.
—北京:中国石化出版社,2002
ISBN 7-80164-291-0

Ⅰ.催… Ⅱ.①卢… ②王… Ⅲ.石油炼制-流化催化裂化
Ⅳ.TE624.4

中国版本图书馆 CIP 数据核字(2002)第 080378 号

中国石化出版社出版发行
地址:北京市东城区安定门外大街 58 号
邮编:100011 电话:(010)84271850
http://www.sinopec-press.com
E-mail:press@sinopec.com.cn
北京精美实华图文制作中心排版
北京金明盛印刷服务有限公司印刷
新华书店北京发行所经销
*
787×1092 毫米 16 开本 17 印张 429 千字
2002 年 11 月第 1 版 2004 年 11 月第 1 版第 2 次印刷
定价:35.00 元

v_1 =0.788m/s
v_2 =0.498m/s
G =81.578t/h
W_i =6.696t
W_c =4.951t
ΔP_r =1314.9mmH$_2$O
$\bar{P}_d$ =194.5kg/m^3
v_1— Regenerator Dense-Phase Linear Velocity
v_2— Regenerator Dilute-Phase Linear Velocity
W— Regenerator Reserve
Ungiven pressure units are 10^5 Pa;all density units are kg/m^3 ,applicable to the following figures

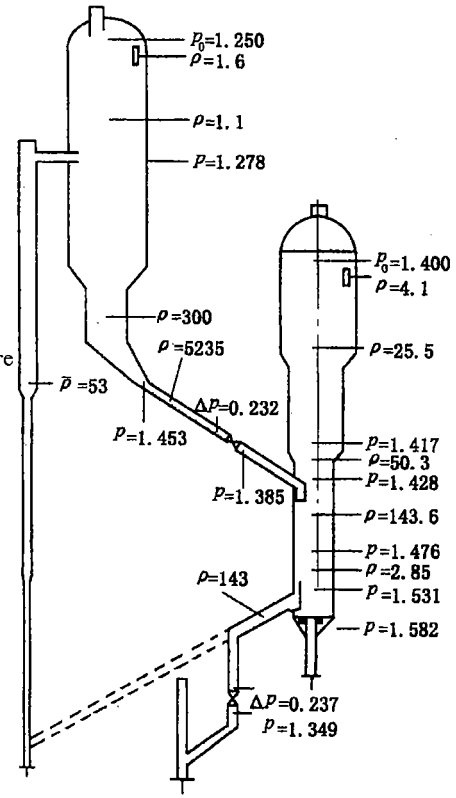

Fig3-3-11(a) Distribution of pressure and density at each point in the system

v_1 =0.808m/s
v_2 =0.504m/s
G =75.129t/h
W_i =7.02t
W_c =5.239t
ΔP_r =1421.6mmH$_2$O
$\bar{\rho}_d$ =198.4kg/m^3

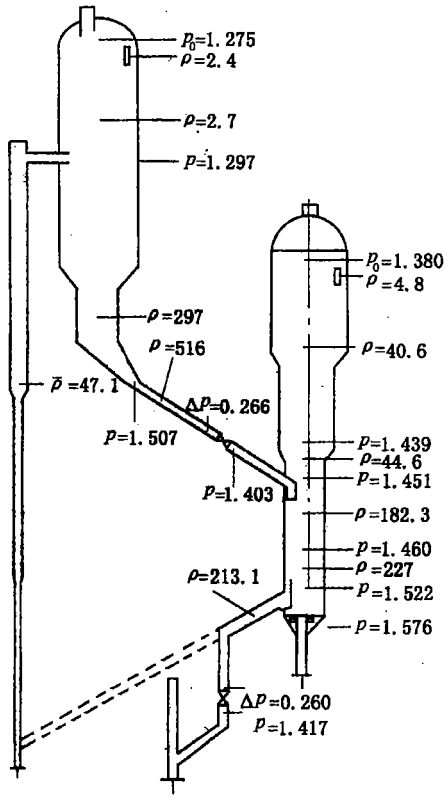

Fig3-3-11(b) Distribution of pressure and density at each point in the system

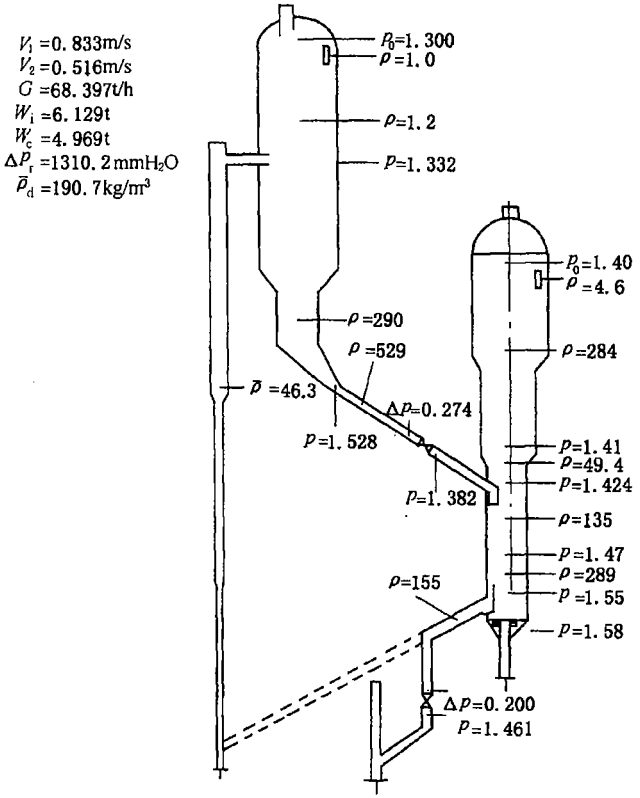

Fig3-3-11(c) Distribution of pressure and density at each point in the system

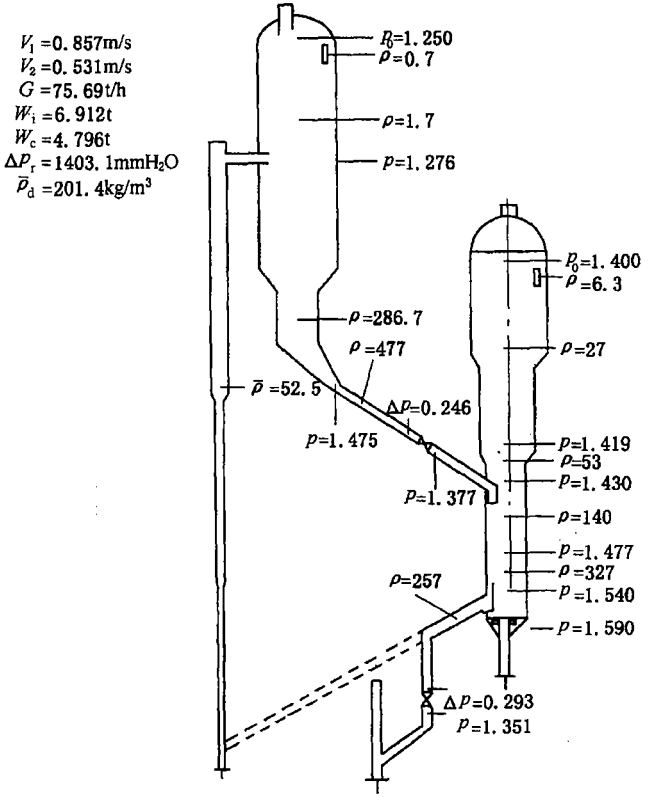

Fig3-3-11(d) Distribution of pressure and density at each point in the system

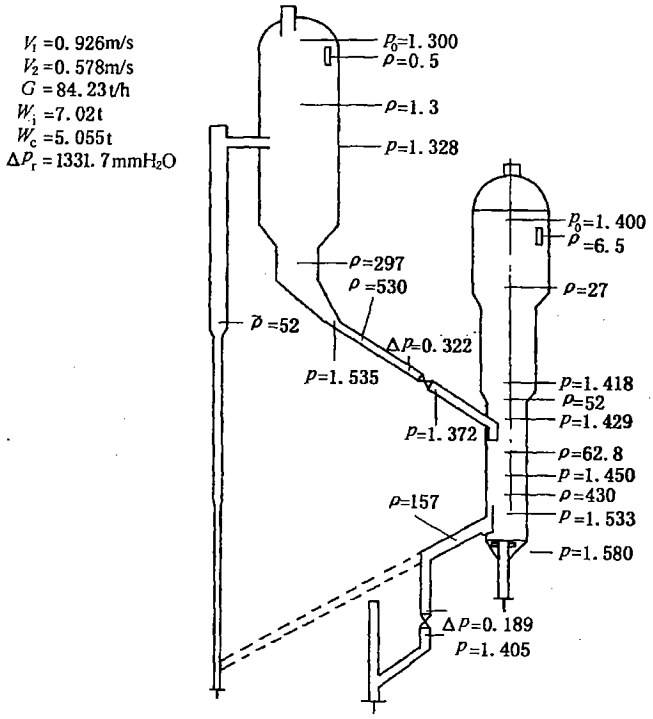

Fig3-3-11(e) Distribution of pressure and density at each point in the system

3.2.3 再生器的催化剂密度分布规律

通过测试所得实际数据，经数据处理，标绘出沿再生器轴向催化剂密度分布曲线，见图3－3－12。

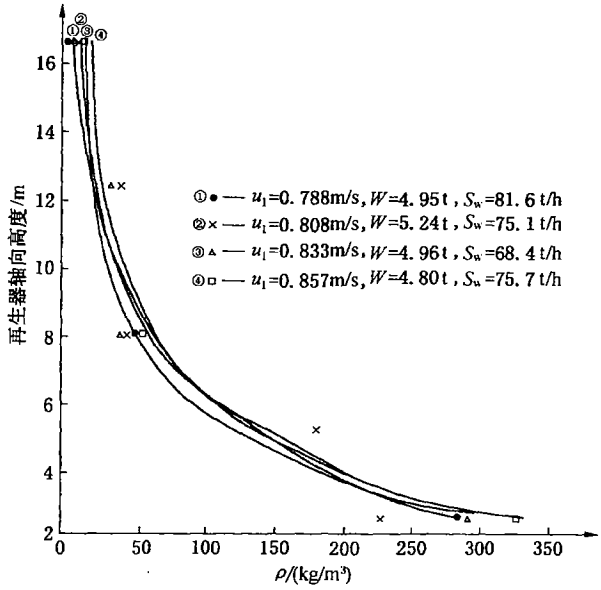

图 3－3－12 再生器密度分布曲线

ANNEX B

ELSEVIER

Chemical Engineering Science 62 (2007) 1184–1198

Chemical Engineering Science

www.elsevier.com/locate/ces

Dynamic modelling of an industrial R2R FCC unit

Joana L. Fernandes[a], Jan J. Verstraete[b], Carla I.C. Pinheiro[a,*], Nuno M.C. Oliveira[c], Fernando Ramôa Ribeiro[a]

[a]*IBB–Institute for Biotechnology and Bioengineering, Centre for Biological and Chemical Engineering, Instituto Superior Técnico, Av. Rovisco Pais, 1049-001 Lisboa, Portugal*

[b]*Institut Français du Pétrole BP 3, 69390 Vernaison, France*

[c]*GEPSI-PSE Group, Department of Chemical Engineering, University of Coimbra, Pinhal de Marrocos, 3030-290 Coimbra, Portugal*

Received 30 December 2005; received in revised form 15 September 2006; accepted 1 November 2006
Available online 10 November 2006

Abstract

The aim of this study is to obtain a model that can simulate the performance of an industrial fluid catalytic cracking (FCC) unit in steady and dynamic state, and which will subsequently be used in studies of control and real time optimisation. In this paper, a dynamic model for a R2R type FCC unit is presented. The model includes the riser, the stripper/disengager, the regeneration system and the catalyst transport lines. Mass, energy and pressure balances are performed for each of these sections.

Simulation results for steady state are presented and compared qualitatively to those obtained from previous FCC models. The dynamic behaviour of the system is explored through two perturbations in open loop, one on the fresh feed flow rate and one on the air flow rate to the first regenerator. The results illustrate the consistency of the model and are in agreement with what has been observed in studies available in the open literature.

Keywords: Fluid catalytic cracking; Mathematical modelling; Dynamic simulation; Nonlinear dynamics

1. Introduction

Fluid catalytic cracking (FCC) is one of the most important processes in a refinery, and is therefore sometimes referred to as the heart of the refinery. Several studies have been made on the modelling, simulation, kinetics, multiplicity of steady states, chaotic behaviour, on-line optimisation and control of FCC units. However, there are still large areas to be examined due to the complexity and to the economical importance of this process.

The initial attempts to model FCC units where primarily oriented towards the kinetics of cracking. The first and most widely used kinetic models are the three lump model proposed by Weekman and Nace (1970), which mainly focused on feedstock conversion and gasoline selectivity, and a 10 lump model that introduced a more chemical description of the heavier fractions, also proposed by Weekman and co-workers a few years later (Jacob et al., 1976). An extended kinetic model that uses 18 lumps to distinguish several chemical groups within each hydrocarbon fraction has been published by Pitault et al. (1994).

More detailed kinetic modelling approaches have also been applied to catalytic cracking. The "Structure Oriented Lumping" approach, described by Quann and Jaffe (1992, 1996) and Christensen et al. (1999), uses an extensive network of reactions between lumps that are represented as an assembly of molecular building blocks. In more recent studies, detailed kinetic models for the catalytic cracking of industrial vacuum gas oil (VGO) feeds have been developed based on the single events approach (Moustafa and Froment, 2003). This modelling technique aims at retaining the full detail of the reaction pathways of all individual feed components and reaction intermediates by describing the reaction network in terms of elementary steps. It therefore requires a very detailed characterisation of feeds and products, which is generally not available in industry, and is computationally more demanding than lumped models. Semi-lumped models that consider the

* Corresponding author. Tel.: +351 21 841 78 87; fax: +351 21 841 91 98.
E-mail address: carla.pinheiro@ist.utl.pt (C.I.C. Pinheiro).

0009-2509/$ - see front matter © 2006 Elsevier Ltd. All rights reserved.
doi:10.1016/j.ces.2006.11.003

reaction types occurring in catalytic cracking have also been proposed, in which the products and reactants are lumped by characteristics such as the carbon number (Pinheiro et al., 1999; Carabineiro et al., 2004). Unfortunately, studies concerning this type of models have been made mainly for model molecules and like the single event models they require good characterisation of the reactants and products.

In FCC modelling, studies of the regenerator hydrodynamics and steady state behaviour have also been conducted early on (Errazu et al., 1979; De Lasa and Grace, 1979). The combustion phenomena in the regenerator, such as the CO post-combustion reaction (Morley and De Lasa, 1988) and the prediction of the CO_2/CO ratio in the flue gas (Weisz, 1966), have been a matter of interest for investigators.

Several authors have presented steady and unsteady state models that describe the riser reactor-regenerator system of a FCC unit. Among these are works by McFarlane et al. (1993), Arbel et al. (1995a), Han and Chung (2001a), Elnashaie et al. (2004) and Secchi et al. (2001), which will be described in more detail.

McFarlane et al. (1993) published a well-detailed model based on the Exxon model IV that covers most parts of a Model IV type FCC unit. However, the model uses an oversimplified cracking kinetic model and it also lacks a description of combustion reactions. Arbel et al. (1995a) developed a model to predict both steady and unsteady states of the current generation of FCC units. For the riser reactor, their model assumed pseudo steady state, plug flow, no slip velocity between the gas and catalyst particles, constant superficial velocity and adiabatic operation. The cracking kinetics were described by means of the 10 lump model proposed by Jacob et al. (1976). The regenerator was modelled according to the two-phase model described in Kunii and Levenspiel (1990). Arbel et al. (1995b) used this model in their study on the multiplicity of steady states and in control applications.

Elnashaie et al. (2004) have recently presented a dynamic model of the riser reactor-regenerator system that is similar to the one developed by Arbel et al. (1995a). In their paper, they mainly focus on bifurcation and multiplicity of steady states in the FCC unit that arise from the highly exothermic combustion reactions and back mixing in the regenerator.

Secchi et al. (2001) presented a model for a stacked UOP FCC unit where the riser is described as a plug flow reactor in dynamic state, however, with no overall mass accumulation. Slip velocity between gas and catalyst was not considered. Two hydrodynamic models were proposed for the regenerator: a CSTR and a two-phase theory model. After comparison of these two approaches, the authors concluded that the CSTR is not able to correctly predict the CO/CO_2 ratio. On the other hand, Errazu et al. (1979) and Vale (2002) also compared steady state results with a two-phase theory model for the regenerator to those obtained with a one-phase model that represents the regenerator as a CSTR. They both concluded that there were no significant differences between the predictions of the two models, which is in disagreement with the conclusions of Secchi et al. (2001).

A quite comprehensive model of the FCC unit was presented by Han and Chung (2001a). Their model describes a FCC unit comprising a riser, stripper/disengager, regenerator and catalyst transport lines with slide valves. Besides the mass and energy balances for the riser, the authors also wrote the momentum equations for the gas and the catalyst particles, which allows determining the velocity profiles along the riser reactor and accounts for the slip velocity between gas and catalyst particles. The authors claim that a deviation in gas oil conversion as high as 9.6% can be obtained by including and excluding the momentum equations in the riser model (Han and Chung, 2001a). In their second paper (Han and Chung, 2001b), however, they present velocity profiles with a slip velocity below 0.25 m/s, corresponding to a slip factor close to 1. This is clearly in disagreement with typical slip factors in the riser of about 2, which have been used by many other authors (Das et al., 2003; Fligner et al., 1994; Malay et al., 1999).

The existence of high slip factors is attributed by Fligner et al. (1994) to the formation of clusters along the riser reactor. A cluster is an aggregate of particles moving together with the same velocity and has a higher "free falling velocity" than the terminal velocity of individual particles. Hence, when the amount of clusters increases, the slip factor between gas and catalyst will also increase. According to Pärssinen (2002), the reported size of FCC catalyst clusters is between 2 and 15 mm. In the dilute region of the riser, however, the probability of cluster formation is smaller due to the higher velocities and the slip factor decreases significantly in this region.

Currently, several types of FCC units are in operation, using various designs. Hence, not all models available in literature can easily be applied for every type of unit. In this study, a dynamic model is presented for an R2R unit comprising a riser, a stripper, a disengager, two standpipes and a regeneration system composed of two regenerators connected by a lift. An effort was made to develop a model that is as simple as possible at the computational level without disregarding important characteristics of the FCC unit, such as its hydrodynamics and a cracking kinetic scheme able to predict the major cracking products: decanted oil (DO) (unconverted vacuum gas oil feed); light cycle oil (LCO), gasoline (GLN), liquefied petroleum gas (LPG), fuel gas (FG) and coke (CK). The riser hydrodynamics accounts for the molar expansion for the gas and considers a force balance on the catalyst particles, which results in a slip velocity between catalyst and gas. For the regenerators, a simple CSTR hydrodynamic model was used; a previous study on R2R units (Vale, 2002) showed the good performance of this model, since there were no significant differences between the steady state behaviour of a two-phase theory model and a CSTR model.

The FCC model was implemented in FORTRAN using a modular approach. A qualitative analysis of steady state results and of the dynamic behaviour has been made, showing promising results for future use of this model in studies of advanced control and real time optimisation.

2. Process description

The R2R resid FCC process, initially devised by Total (Dean et al., 1982a,b) and now licensed by Axens/IFP and

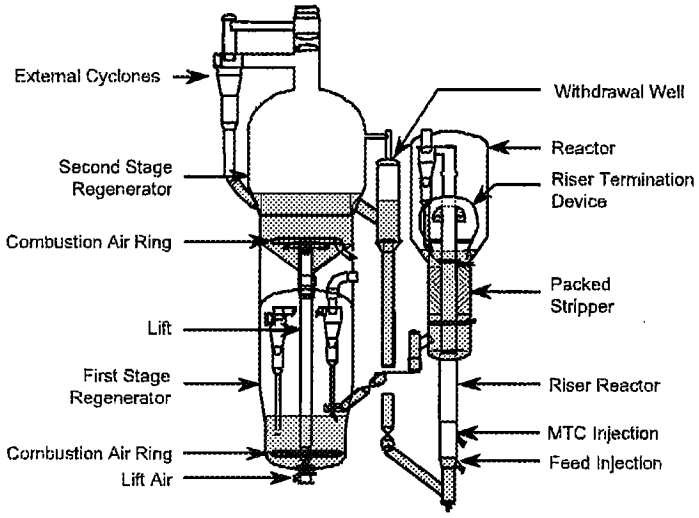

Fig. 1. R2R fluid catalytic cracking process (adapted from Gauthier et al., 2000).

Stone & Webster (Marcilly and Bonifay, 1996; Letzsch and Jackson, 2004), consists of a riser reactor, a stripper and two regenerators. The two-regenerator R2R technology allows to process feeds with a high residue content, as more coke can be burnt. In this configuration, the first regenerator (regenerator 1) acts as a mild pre-combustion zone that removes 40–70% of the coke on the catalyst. The partially regenerated catalyst with less than 0.5 wt% coke is then air-lifted to the elevated second regenerator (regenerator 2), where complete regeneration is achieved with slight air excess and under a low steam partial pressure in order to minimise catalyst deactivation (Gauthier et al., 2000). A schematic of a typical R2R resid FCC unit is shown in Fig. 1.

The regenerated catalyst flows through the standpipe from the regenerator to the bottom of the riser. After a short reacceleration zone to stabilise the catalyst flow, preheated finely atomised oil feed is injected onto the hot catalyst. Upon contacting the catalyst, the feed vaporises and cracking starts. Vaporisation and cracking generates a significant expansion that lifts the catalyst up the riser. As the cracking reactions proceed throughout the riser, heavy hydrocarbons are cracked into desired products, but large amounts of coke, 4–8 wt% of the feed, are simultaneously deposited on the catalyst, reducing its activity.

At the end of the riser, a riser termination device rapidly separates hydrocarbon vapours and catalyst particles to reduce further thermal and catalytic cracking. This section is composed of a stripper, in which steam is used to remove most of the entrained hydrocarbon vapours in a counter-current dense phase stripper with multiple steam injections, and of a disengagement vessel with cyclones that ensure an efficient separation of the entrained catalyst particles. The stripped spent catalyst is then introduced on top of the first regenerator fluidised bed, where the hot flue gas provides ultimate stripping.

In the fluidised bed regenerator, the catalyst activity is restored by combusting the coke in air. Besides restoring the catalyst activity, the combustion process also raises the catalyst temperature, thus providing the necessary energy to the vaporisation of the feed and the cracking reactions in the riser. Inside the regenerator, two distinct regions can be observed: the dense region and the dilute region, frequently termed freeboard. The dense region concentrates most of the solids and is the phase where most of the combustion occurs. At the surface of the dense fluidised bed, bubbles erupt, ejecting particles into the dilute phase freeboard, where the solids concentration decreases sharply with height towards a very low catalyst concentration (De Lasa and Grace, 1979).

The transport of catalyst particles from the stripper to the regenerator and from the regenerator to the riser bottom is achieved by means of two standpipes. Smooth operation of these standpipes is critical to an FCC unit, since the standpipes link riser and regenerator. It is also important to note that the catalyst flows to the riser and to the regenerator are controlled by a slide valve positioned in each standpipe. The opening of these valves controls the catalyst circulation rate through the entire FCC unit.

3. Mathematical model

The mathematical model presented here describes the steady state and dynamic behaviour of a R2R industrial unit. The main assumptions are instantaneous and complete feed vaporisation, pseudo-steady state for the riser, which is modelled as an adiabatic plug flow reactor with a six-lump kinetic model, a CSTR dynamic model for the stripping/disengagement vessel and a CSTR dynamic model to describe each regenerator. The lift between the regenerators is also modelled as a plug flow reactor in pseudo-steady state. The catalyst circulation rate through each standpipe is determined by the

pressure drop across a slide valve and is given by a valve equation.

3.1. Feed vaporisation

According to Ali and Rohani (1997), the inlet zone is the most complex part of the riser, since there is high turbulence, flow inhomogeneity and large temperature and concentration gradients. However, the same author also indicates that the feed takes only about 3% of the mixture residence time to vaporise completely, which justifies the assumption of instantaneous vaporisation.

As the vaporisation is assumed to be instantaneous and complete, the energy balance will be written in the steady state without any heat transfer resistances. The change in feed enthalpy during vaporisation is given by the correlations in Montgomery (1993) that depend on the feed characteristics and can be found in the Appendix.

3.2. Riser

The riser hydrodynamics is modelled as a plug flow reactor with a one-dimensional model that only considers axial variations of the variables and diffusional and turbulent transport of mass, momentum, and heat are neglected. An hybrid model was used to describe gas and solid velocity along the riser. The gas phase was modelled as a continuum phase and the continuity equation that expresses molar expansion was used to obtain the gas velocity profile. For the solids phase, it was considered that all FCC particles are identical and Newton's second law of motion was used to write a force balance over a particle.

For concentration and temperature; both internal and external mass- and heat-transport resistances were neglected, and these variables are modelled considering a pseudo-homogeneity assumption.

The cracking kinetics is described by a six-lump model for gas oil cracking adapted from the model first presented by Takatsuka et al. (1987) with a deactivation function depending on the catalyst coke content (Vale, 2002). The lumps considered are VGO + DO(> 360°C); LCO (220–360 °C); GLN (C5–220 °C); LPG (C3 and C4); FG (H2, C1, C2 and H2S) and coke. The reactions between these lumps are presented in Fig. 2. Similarly to other authors (Ancheyta-Juárez et al., 1999; Corella and Frances, 1991; Hagelberg et al., 2002) gasoline and gases conversion to coke were not considered since the kinetic constants for these reactions are negligible in comparison to the other reactions.

Except for the second order VGO cracking reactions, all reactions are first order. The kinetic parameters were determined from pilot plant data.

According to this kinetic model, the rate of the reaction of lump i towards lump j is given by

$$\hat{r}_{ij} = \Phi A_{ij} \exp\left(-\frac{E_{ij}}{RT}\right) \hat{C}_i^{n_{ij}}, \tag{1}$$

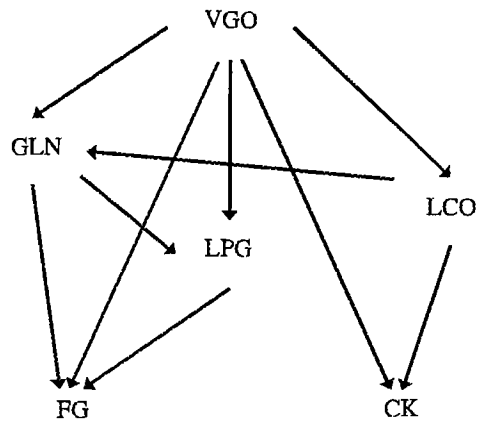

Fig. 2. Kinetic scheme of the cracking reactions taking place in the riser (adapted from Takatsuka et al., 1987).

with Φ the deactivation function, which is given by

$$\Phi = \exp(-\alpha Y_{ck}^{cat}). \tag{2}$$

Mass balances for each lump and for the coke content on the catalyst are given by

$$\varepsilon_g \Omega_{RS} \frac{\partial \hat{C}_i}{\partial t} + \frac{\partial \hat{F}_i}{\partial z} = \Omega_{RS}(1-\varepsilon_g)\hat{r}_i, \tag{3}$$

$$\hat{r}_i = \sum_j \hat{r}_{ji} - \sum_j \hat{r}_{ij}, \tag{4}$$

$$\varepsilon_c \Omega_{RS} \rho_c \frac{\partial Y_{ck,RS}^{cat}}{\partial t} + \frac{\partial F_{ck}}{\partial z} = \Omega_{RS} \varepsilon_c \hat{r}_{ck}. \tag{5}$$

The coke deposited on the catalyst can be of two different natures: catalytic coke that results from secondary catalytic reactions and CCR coke which results from thermal decomposition of heavy compounds that are present in the feed. According to Arbel et al. (1995a), CCR coke deposits almost immediately on the catalyst surface. However, since this coke is not directly formed at a catalytic site and is mainly deposited on the catalyst matrix, it is considered that it does not contribute to catalyst deactivation. From the total amount of CCR present in the feed, only a fraction x_{CCR} is converted into coke. The following balance then gives the total amount of coke on the catalyst in the riser:

$$Y_{ck,RS} = Y_{ck,RS}^{cat} + Y_{ck}^{CCR} \tag{6}$$

with

$$Y_{ck}^{CCR} = \frac{F_g^{CCR} x_{CCR}}{F_c}. \tag{7}$$

Gas molar expansion as well as slip velocity between gas and solids is accounted for in the riser model. Formation of clusters of catalyst particles has also been considered, since several papers show evidence of this phenomenon for FCC catalysts (Fligner et al., 1994; Pärssinen, 2002). The size of a cluster was

determined by using the correlation from Xu and Kato (1999) that can be found in Appendix. The molecular weights of the lumps needed to predict gas molar expansion were taken from Pitault et al. (1994).

To derive the velocity profile for the gas phase the continuity equation as a molar balance was written as already mentioned.

$$\varepsilon_g \frac{\partial(\sum_i C_i)}{\partial t} + \frac{\partial(\varepsilon_g v_g \sum_i C_i)}{\partial z} = (1-\varepsilon_g)\sum_i \frac{\hat{r}_i}{M_{w,i}}, \tag{8}$$

$$\frac{\partial v_g}{\partial z} = \frac{1-\varepsilon_g}{\varepsilon_g C_t}\sum_i r_i - \frac{v_g}{C_t}\frac{\partial C_t}{\partial z} - \frac{v_g}{\varepsilon_g}\frac{\partial \varepsilon_g}{\partial z} - \varepsilon_g \frac{\partial C_t}{\partial t}, \tag{9}$$

$$C_t = \sum_i \frac{\hat{C}_i}{M_{w,i}}, \tag{10}$$

$$\frac{\partial C_t}{\partial t} = \sum_i \left[\frac{\partial \hat{C}_i}{\partial t} \times \frac{1}{M_{w,i}}\right]. \tag{11}$$

For the gas phase it is assumed that hydrocarbon vapours behave like an ideal gas and the ideal gas law is used for total concentration calculations.

$$P = C_t RT \tag{12}$$

$$\frac{\partial C_t}{\partial z} = \frac{1}{RT}\frac{\partial P_{RS}}{\partial z} - \frac{C_t}{T}\frac{\partial T_{RS}}{\partial z}. \tag{13}$$

For the solid phase, a force balance was done over a cluster of FCC particles. The movement of a FCC cluster is then given by the equation of Newton (Pugsley and Berruti, 1996; Sabbaghan et al., 2004):

$$\rho_c \frac{\pi d_{cl}^3}{6}\frac{\partial v_c}{\partial t} = C_D \frac{\rho_g (v_g - v_c)^2}{2}\frac{\pi d_{cl}^2}{4} + \rho_g \frac{\pi d_{cl}^3}{6} g - \rho_c \frac{\pi d_{cl}^3}{6} g. \tag{14}$$

The drag coefficient, C_D, for the gas–solid interphase friction is given in Appendix.

Considering the equality:

$$\frac{\partial v_c}{\partial t} = \frac{\partial z}{\partial t} \times \frac{\partial v_c}{\partial z} \quad \Leftrightarrow \quad \frac{\partial v_c}{\partial t} = v_c \frac{\partial v_c}{\partial z}. \tag{15}$$

Eq. (14) can be rearranged to give the velocity profile along the riser for the solid phase:

$$\frac{\partial v_c}{\partial z} = C_D \frac{3}{4}\frac{\rho_g (v_g - v_c)^2}{d_{cl}\rho_c v_c} + \frac{(\rho_g - \rho_c) g}{\rho_c v_c}. \tag{16}$$

For the energy balance the riser was considered as an adiabatic plug flow reactor without heat transfer resistances between gas and solid phases. An overall cracking enthalpy expressed per unit mass of VGO converted covers the overall heat consumed by the endothermic cracking reactions. Due to the assumption of pseudo-homogeneity for the energy balance both gas and solids share the same temperature (Das et al., 2003).

$$\rho_m C_{p,m}\frac{\partial T_{RS}}{\partial t} + \frac{F_g C_{p,g} + F_c C_{p,c}}{\Omega_{RS}}\frac{\partial T_{RS}}{\partial z} = \varepsilon_c \Delta H_{crk} \hat{r}_{DO}, \tag{17}$$

$$\rho_m C_{p,m} = \varepsilon_g \rho_g C_{p,g} + \varepsilon_c \rho_c C_{p,c}. \tag{18}$$

Pressure profile along the riser is given by the total momentum balance for both gas and solid phase (Arastoopour and Gidaspow, 1979).

$$\frac{\partial P_{RS}}{\partial z} = -(\varepsilon_c \rho_c + \varepsilon_g \rho_g) g - \frac{\partial}{\partial z}[\rho_g \varepsilon_g v_g^2 + \rho_c (1-\varepsilon_g) v_c^2] - F_w. \tag{19}$$

Pugsley and Berruti (1996) showed that the total pressure drop per unit length along the riser in fully developed flow can be approximated by the pressure drop caused by hydrostatic head of solids and that the acceleration effects are important only at the base of the riser. Frictional effects due to solid friction and gas friction with the riser walls, F_w, can then be neglected.

$$\frac{\partial P_{RS}}{\partial z} = -(\varepsilon_c \rho_c + \varepsilon_g \rho_g) g - \frac{\partial}{\partial z}[\rho_g \varepsilon_g v_g^2 + \rho_c (1-\varepsilon_g) v_c^2]. \tag{20}$$

The void fractions of the solid and gas phases are given by the following definitions:

$$\varepsilon_c = \frac{F_c}{v_c \rho_c \Omega_{RS}}, \tag{21}$$

$$\varepsilon_g = 1 - \varepsilon_c. \tag{22}$$

For dynamic simulation purposes the riser is considered to be in pseudo-steady state, since it has a residence time of the order of a few seconds (2–5 s), while the regenerators and the stripper have characteristic times in the order of a few minutes. It was then considered that the regenerators and stripper vessels control the transient response of the system reactor-regenerator when perturbations to the system occur.

3.3. Stripper/disengager

In recent years many developments have been made in the design of riser termination devices in order to achieve a better separation of the gas and solid phases and to reduce overcracking of gasoline into lighter components. In this work, it will be assumed that the separation of gases and solids is fast and efficient so there are no reactions occurring in the disengager/stripper section, which will be modelled as a continuous stirred tank (CST) in unsteady state. The properties of the catalyst bed will be determined by considering that the fluidised stripper bed is at incipient fluidisation. Since the catalyst level in the stripper is an important variable for the control of the FCC unit, the variations of the stripper bed level will be accounted for (Eq. (24)–(26)).

It is also assumed that a percentage of hydrocarbons remains adsorbed/occluded in the catalyst pores after stripping. This is the so-called cat-to-oil coke (Montgomery, 1993). An empirical stripping function based on pilot plant data, given in Appendix is proposed for predicting cat-to-oil coke.

Coke mass balance:

$$\frac{\partial Y_{ck,ST}}{\partial t} = \frac{F_{c,RSout} Y_{ck,RSout} - F_{c,STout} Y_{ck,ST}}{W_{c,ST}}. \tag{23}$$

Catalyst inventory:

$$\frac{\partial W_{c,\mathrm{ST}}}{\partial t} = F_{c,\mathrm{RSout}} - F_{c,\mathrm{STout}}, \tag{24}$$

$$\partial W_{c,\mathrm{ST}} = \rho_c \varepsilon_c \Omega_{\mathrm{ST}} \partial L_{\mathrm{ST}}, \tag{25}$$

$$\frac{\partial L_{\mathrm{ST}}}{\partial t} = \frac{F_{c,\mathrm{RSout}} - F_{c,\mathrm{STout}}}{\rho_c \varepsilon_c \Omega_{\mathrm{ST}}}. \tag{26}$$

Gas inventory:

$$\frac{\partial W_{g,\mathrm{ST}}}{\partial t} = F_{g,\mathrm{RSout}} + F_s - F_{g,\mathrm{STout}}. \tag{27}$$

The gas flow rate at the disengager outlet is determined by the opening of the valve to the main fractionator, which depends on the pressure in the stripper and in the main fractionator. The gas flow rate is therefore given by the following equation:

$$F_{g,\mathrm{STout}} = k_{v,MF}(x_v)\sqrt{P_{g,\mathrm{ST}} - P_{g,\mathrm{MF}}} \tag{28}$$

The catalyst flow rate leaving the stripper towards the regenerator is controlled by a slide valve in the spent catalyst standpipe and the pressure difference between these two vessels:

$$F_{c,\mathrm{STout}} = F_{c,\mathrm{SP}_S} = k_{v,\mathrm{SP}_S}(x_v)\sqrt{\Delta P_{\mathrm{SP}_S}} \tag{29}$$

$$\Delta P_{\mathrm{SP}_S} = P_{\mathrm{ST}_{\mathrm{bottom}}} + \rho_c \varepsilon_c L_{\mathrm{SP}_S} \sin\theta_{\mathrm{SP}_S} g - P_{\mathrm{RG1}} \tag{30}$$

The pressure in the disengagement vessel is calculated by assuming ideal gas behaviour for the hydrocarbon vapours:

$$P_{g,\mathrm{ST}} = W_{g,\mathrm{ST}} \frac{RT_{g,\mathrm{ST}}}{M_{w,g,\mathrm{ST}} V_{g,\mathrm{ST}}} Z_{g,\mathrm{ST}}, \tag{31}$$

$$V_{g,\mathrm{ST}} = V_{\mathrm{ST}} - \frac{W_{c,\mathrm{ST}}}{\rho_c}. \tag{32}$$

The pressure at the bottom of the disengager/stripper section is higher than at the top, due to the static head exerted by the catalyst. This is given by

$$P_{\mathrm{ST}_{\mathrm{bottom}}} = P_{g,\mathrm{ST}} + \rho_c g L_{\mathrm{ST}}. \tag{33}$$

The energy balance is written by assuming thermal equilibrium between the outlet streams, neglecting any heat transfer with the exterior. The heat of desorption will also be neglected.

$$\begin{aligned}\frac{\partial(W_{c,\mathrm{ST}} C_{p_c} T_{\mathrm{ST}} + W_{g,\mathrm{ST}} C_{p_g} T_{\mathrm{ST}})}{\partial t} &= F_{g,\mathrm{RSout}} \mathrm{H}_{g,\mathrm{RSout}} \\ &+ F_{s,\mathrm{ST}} \mathrm{H}_{s,\mathrm{ST}} + F_{c,\mathrm{RSout}} \mathrm{H}_{c,\mathrm{RSout}} \\ &- F_{g,\mathrm{STout}} \mathrm{H}_{g,\mathrm{STout}} - F_{c,\mathrm{STout}} \mathrm{H}_{c,\mathrm{STout}},\end{aligned} \tag{34}$$

$$\mathrm{H}_k = \bar{C}_{p_k} \times (T_k - T_{\mathrm{ref}}) \tag{35}$$

3.4. Regenerators

FCC regenerators consist of large fluidised bed reactors, where the strongly exothermic combustion reactions take place. In this study, the freeboard will be neglected and the dense phase will be modelled as a CSTR.

Coke is considered to be composed of carbon and hydrogen, although in practice sulphur and nitrogen are also present in small quantities. Moreover, no distinction is made between different types of coke with respect to its combustion. This last assumption might be subject to some discussion, as we consider that gaseous hydrocarbons entrained with the catalyst (soft coke) burn in the same way as hard coke, which is a solid deposited on the catalyst.

The combustion kinetics considered in this work was taken from previous studies at IFP (Daly et al., 2001; Vale, 2002; Zwinkels and Nougier, 1997). The combustion of carbon can be written as the following overall reaction:

$$\mathrm{C} + \left(\frac{\sigma + 1/2}{\sigma + 1}\right)\mathrm{O_2} \rightarrow \left(\frac{\sigma}{\sigma + 1}\right)\mathrm{CO_2} + \left(\frac{1}{\sigma + 1}\right)\mathrm{CO}. \tag{36}$$

The combustion of carbon produces both CO_2 and CO in a proportion of σ. The CO_2/CO ratio σ is very important, since it affects both the mass and energy balances in the regenerator. Indeed, the heat of combustion to CO_2 is almost 3 times the heat of combustion to CO, which means that the CO_2/CO ratio controls the heat balance in the regenerator (Arbel et al., 1995a).

Several correlations have been derived to calculate σ, but the one proposed by Arthur (1951) is the most quoted in the literature. Arthur's correlation states that σ decreases exponentially with temperature. Experimental work done at IFP (Daly et al., 2001; Zwinkels and Nougier, 1997), however, has shown that the carbon combustion rate and the σ ratio are affected by other variables than the temperature, such as water concentration, coke conversion and metals content.

$$\mathrm{C} + \tfrac{1}{2}\mathrm{O_2} \xrightarrow{1,\mathrm{gas\text{–}solid}} \mathrm{CO}, \tag{37}$$

$$r_1^s = r_{\mathrm{C}}\left(\frac{1}{1+\sigma}\right), \tag{38}$$

$$\mathrm{C} + \mathrm{O_2} \xrightarrow{2,\mathrm{gas\text{–}solid}} \mathrm{CO_2}, \tag{39}$$

$$r_2^s = r_{\mathrm{C}}\left(\frac{\sigma}{1+\sigma}\right), \tag{40}$$

$$r_{\mathrm{C}} = (V_{\mathrm{dry}} + V_{\mathrm{wet}})Y_C, \tag{41}$$

$$V_{\mathrm{dry}} = k_{\mathrm{C1}}^{\mathrm{dry}} \exp\left(-\frac{E_{\mathrm{C1}}^{\mathrm{dry}}}{RT}\right) P_{\mathrm{O_2}}^{0.78}, \tag{42}$$

$$V_{\mathrm{wet}} = k_{\mathrm{C1}}^{\mathrm{wet}} \exp\left(-\frac{E_{\mathrm{C1}}^{\mathrm{wet}}}{RT}\right) \times \frac{P_{\mathrm{H_2O}} P_{\mathrm{O_2}}^{0.84}}{P_{\mathrm{O_2}}^{0.84} + k_{\mathrm{C2}}^{\mathrm{wet}} \exp(-E_{\mathrm{C2}}^{\mathrm{wet}}/RT) P_{\mathrm{H_2O}}}, \tag{43}$$

$$\sigma = \sigma_{\mathrm{dry}} \sigma_{\mathrm{wet}}, \tag{44}$$

$$\sigma_{\mathrm{wet}} = 1 + \frac{V_{\mathrm{wet}}}{k_{\mathrm{C3}}^{\mathrm{wet}} \exp(-E_{\mathrm{C3}}^{\mathrm{wet}}/RT) P_{\mathrm{O_2}}^{0.1}} \tag{45}$$

$$\sigma_{\mathrm{dry}} = \frac{P_{\mathrm{O_2}}^{0.11}}{k_{\mathrm{C2}}^{\mathrm{dry}} \exp(-E_{\mathrm{C2}}^{\mathrm{dry}}/RT) f(X_{\mathrm{C}})}. \tag{46}$$

The subscripts *dry* and *wet* represent the partial contributions due to dry and wet conditions during coke combustion, while $f(X_C)$ is a function of carbon conversion. The kinetic constants were determined at IFP (Daly et al., 2001) and are given in Table 4.

In most models, the hydrogen combustion reaction is generally disregarded. However, according to Faltsi-Saravelou and Vasalos (1991), this reaction has to be considered since it has a significant thermal effect. In this study, the rate expression for the hydrogen combustion reaction obtained by Wang et al. (1986) will be used.

$$\mathrm{H} + \tfrac{1}{4}\mathrm{O_2} \xrightarrow{3,\text{gas–solid}} \tfrac{1}{2}\mathrm{H_2O}, \tag{47}$$

$$r_3^s = k_3^s \exp\left(-\frac{E_{a3}^s}{RT}\right) P_{\mathrm{O_2}} Y_{\mathrm{H}}. \tag{48}$$

The carbon combustion reactions produce simultaneously CO_2 and CO. However, the CO produced undergoes further oxidation to CO_2 through the so-called after-burning reactions. The oxidation of CO to CO_2 can be of two different natures: heterogeneous (catalytic) or homogeneous combustion.

$$\mathrm{CO} + \tfrac{1}{2}\mathrm{O_2} \xrightarrow{4,\text{gas–solid}} \mathrm{CO_2}, \tag{49}$$

$$\mathrm{CO} + \tfrac{1}{2}\mathrm{O_2} \xrightarrow{1,\text{gas}} \mathrm{CO_2}. \tag{50}$$

In this work, the following rate expression for the heterogeneous combustion, determined at IFP by Daly et al. (2001), will be used:

$$r_4^s = k_4^s \exp\left(-\frac{E_{a4}^s}{RT}\right) P_{\mathrm{O_2}}^{0.50} P_{\mathrm{CO}}^{0.49} P_{\mathrm{H_2O}}^{-0.26}. \tag{51}$$

The homogeneous conversion of CO to CO_2 is a free radical reaction which is inhibited by the presence of surfaces such as the catalyst (Arbel et al., 1995a). The rate expression used in this study was obtained by Zwinkels and Nougier (1997).

$$r_1^g = \frac{k_1^g \exp(-E_{a1}^g/RT)}{T^{2.1}} y_{\mathrm{O_2}}^{0.6} y_{\mathrm{CO}} y_{\mathrm{H_2O}}^{0.5}. \tag{52}$$

The CSTR regenerator model can now be described as follows:

Gaseous species molar balance:

$$V_{\mathrm{bed}} \frac{\partial C_{i,\mathrm{RG}}}{\partial t} = N_{i,\mathrm{RGin}}^g - N_{\mathrm{total,RGout}}^g \times C_{i,\mathrm{RG}} + V_{\mathrm{bed}} \left(\varepsilon_g \sum_j (r_j^g v_{ji}^g) + \varepsilon_c \rho_c \sum_j (r_j^s v_{ji}^s)\right) \tag{53}$$

Carbon and hydrogen mass balance:

$$\frac{W_{c,\mathrm{RG}}}{M_{w,i}} \frac{\partial Y_{i,\mathrm{RG}}}{\partial t} = \frac{F_{c,\mathrm{RGin}}}{M_{w,i}} Y_{i,\mathrm{RGin}} - \frac{F_{c,\mathrm{RGout}}}{M_{w,i}} Y_{i,\mathrm{RG}} + V_{\mathrm{bed}} \varepsilon_c \rho_c \sum_j (r_j^s v_{ji}^s) \quad i = \mathrm{C \text{ or } H}. \tag{54}$$

Catalyst inventory:

$$\frac{\partial L_{\mathrm{RG}}}{\partial t} = \frac{F_{c,\mathrm{RGin}} - F_{c,\mathrm{RGout}}}{\rho_c \varepsilon_c \Omega_{\mathrm{RG}}}. \tag{55}$$

Gas inventory:

$$\frac{\partial W_{g,\mathrm{RG}}}{\partial t} = F_{g,\mathrm{RGin}} - F_{g,\mathrm{RGout}} + \sum_i (F_{c,\mathrm{RGin}} Y_{i,\mathrm{RGin}}) - \sum_i (F_{c,\mathrm{RGout}} Y_{i,\mathrm{RG}}). \tag{56}$$

Energy balance:

$$\frac{\partial (W_c C_{p_c} T_{\mathrm{RG}} + W_{g,\mathrm{RG}} C_{p_g} T_{\mathrm{RG}})}{\partial t} = F_{g,\mathrm{RGin}} \mathrm{H}_{g,\mathrm{RGin}} + F_{c,\mathrm{RGin}} \mathrm{H}_{c,\mathrm{RGin}} + Q_r^\circ - F_{g,\mathrm{RGout}} \mathrm{H}_{g,\mathrm{RGout}} - F_{c,\mathrm{RGout}} \mathrm{H}_{c,\mathrm{RGout}}. \tag{57}$$

Pressure: The pressure in the dilute phase of the regenerators is given by the ideal gas law, while for the pressure at the bottom, the hydrostatic pressure exerted by the catalyst bed at the bottom of the regenerators is considered.

$$P_{\mathrm{RG_{bottom}}} = P_{g,\mathrm{RG}} + \rho_c \varepsilon_c L_{\mathrm{RG}} g. \tag{58}$$

The catalyst flow rate that passes through the standpipe that links the second regenerator to the riser is then given by

$$F_{c,\mathrm{RG2out}} = F_{c,\mathrm{SP}_R} = k_{v,\mathrm{SP}_R}(x_v)\sqrt{\Delta P_{\mathrm{SP}_R}}, \tag{59}$$

$$\Delta P_{\mathrm{SP}_R} = P_{\mathrm{RG2}} + \rho_c \varepsilon_c L_{\mathrm{SP}_R} \sin\theta_{\mathrm{SP}_R} g - P_{\mathrm{RS_{bottom}}}. \tag{60}$$

The gas flow rate exiting from the regenerator depends on the pressure difference between the flue gases coming out from the regenerators and the pressure inside the regenerator.

$$F_{g,\mathrm{RGout}} = k_{v,\mathrm{RG}}(x_v)\sqrt{P_{g,\mathrm{RG}} - P_{g,\mathrm{SG}}}. \tag{61}$$

3.5. Lift

The two regenerators are linked by a lift that transports catalyst from the lower regenerator to the upper one. Since the residence time of the gas and catalyst in the lift is of the order of a few seconds, pseudo-steady state will be considered as for the riser. It was assumed that both gas and catalyst are in plug flow with combustion reactions occurring.

Gaseous species molar balance:

$$\varepsilon_g \Omega_{\mathrm{Lift}} \frac{\partial (C_i)}{\partial t} + \frac{\partial N_{i,\mathrm{Lift}}^g}{\partial z} = \Omega_{\mathrm{Lift}} \left(\varepsilon_g \sum_j (r_j^g v_{ji}^g) + \varepsilon_c \rho_c \sum_j (r_j^s v_{ji}^s)\right). \tag{62}$$

Carbon and hydrogen molar balance:

$$\frac{\varepsilon_c \rho_c \Omega_{\mathrm{Lift}}}{M_{w,i}} \frac{\partial (Y_i)}{\partial t} + \frac{\partial N_{i,\mathrm{Lift}}^s}{\partial z} = \Omega_{\mathrm{Lift}} \varepsilon_c \rho_c \sum_j (r_j^s v_{ji}^s). \tag{63}$$

Energy balance:

$$\rho_m C_{p,m} \Omega_{\mathrm{Lift}} \frac{\partial T_{\mathrm{Lift}}}{\partial t} + \sum_i F_i C_{p_i} \frac{\partial T_{\mathrm{Lift}}}{\partial z} = -\Omega_{\mathrm{Lift}} \left(\varepsilon_g \sum_j (r_j^g \Delta \mathrm{H}_j^g) + \varepsilon_c \rho_c \sum_j (r_j^s \Delta \mathrm{H}_j^s)\right). \tag{64}$$

Since the molar expansion is negligible in the lift, no velocity profiles were calculated and the porosity in the lift is given by an empirical correlation available at IFP (Vale, 2002).

$$\varepsilon_g = 1 - \frac{2.06 G_c \exp(-0.251 u_g)}{\rho_c}, \tag{65}$$

where G_c is catalyst flux and u_g is the gas superficial velocity:

$$G_c = \frac{F_c}{\Omega_{\text{Lift}}}, \tag{66}$$

$$u_g = \frac{F_g}{\rho_g \Omega_{\text{Lift}}}. \tag{67}$$

4. Numerical and computational methods

The mathematical model of an industrial FCC unit presented in this paper corresponds to a large system of differential and algebraic equations. To solve this problem, the model was implemented in FORTRAN using a modular approach.

Each module corresponds to a section of the unit that is solved at each time integration step by an appropriate numerical method. The solvers used in this study were:

- ZEROIN—used to find the roots of nonlinear algebraic equations based on Brent's algorithm (Brent, 1971).
- LSODE—used to solve systems of ordinary differential equations (ODE) based on the Gear's algorithm (Hindmarsh, 1980; Radhakrishnan and Hindmarsh, 1993).
- DASPK—used to solve systems of differential algebraic equations (DAE) based on the Petzold-Gear's BDF algorithm (Li and Petzold, 1999).

Initial and boundary conditions were estimated through steady state simulation for a base case of typical industrial operating conditions. The operating conditions for this base case are presented in Table 1. The R2R dimensions used for simulation are presented in Table 2 and feedstock and catalyst properties are listed in Table 3. Finally, the kinetic data used for simulation is listed both for cracking reactions and combustion reactions in Table 4 .

Table 1
R2R base case operating conditions

Base case operating conditions	
Fresh feed flowrate (kg/s)	60.82
Fresh feed temperature (K)	450.15
Steam flowrate entering the riser (kg/s)	3.58
Steam temperature (K)	592.25
Catalyst-to-oil ratio, C/O (kg/kg)	6.9
Stripping steam (kg/s)	2.08
Stripping steam temperature (K)	592.25
Air to regenerator 1 (kg/s)	30.71
Air to regenerator 2 (kg/s)	11.19
Air to lift (kg/s)	4.8
Air temperature (K)	428.15
Pressure in the main fractionator (Pa)	1.1×10^5
Pressure of the flue gases (Pa)	1.1×10^5

Table 2
Dimensions of the simulated R2R industrial unit

	R2R unit dimensions	
	Length (m)	Diameter (m)
Riser	32.11	1.6
Stripper	8.0	3.6
Disengager	8.5	5.1
Regenerator 1	13.7	6.4
Regenerator 2	11.8	5.9
Lift	20.64	0.8
Spent catalyst standpipe	8.5	0.8
Regenerated catalyst standpipe	7.5	0.8

Table 3
Feed and catalyst properties

Feedstock properties	
API (°)	20.0
Watson characterisation factor, K_W (dimensionless)	11.9
Conradson Carbon residue, CCR (wt%)	5.78
Fraction of CCR converted in coke, x_{CCR}	0.31
Coke composition	$CH_{0.8}$
Specific heat, C_{pHC} (J/(kg K))	1255.5
Heat of reaction, ΔH_{crk} (J/kg VGO)	4.25×10^5
Catalyst properties	
Average particle diameter, d_p (m)	7.4×10^{-5}
Cluster diameter, d_{cl} (m)	2.0×10^{-3}
Density, ρ_c (kg/m^3)	1450
Specific heat, C_{pc} (J/(kg K))	1197.5

5. Simulation results and discussion

In this section, the simulation results for the steady and dynamic states are presented and discussed. Fig. 3 shows the influence of the steady state catalyst-to-oil ratio (COR) on several process variables. It can be seen that increasing the COR leads to an increase in riser outlet temperature. Since a higher flow rate of catalyst enters the riser for a given hydrocarbon flow rate, this also contributes to a higher conversion of the feed as the curve for VGO yield in Fig. 3b shows. Despite a slight increase in coke yield (CK in Fig. 3b), the increase in COR leads to a lower coke content on the spent catalyst. This decrease in catalyst coke content leads to lower regenerator temperatures (RG_1 and RG_2, Fig. 3a), in spite of a slight increase in overall heat release in the regenerators. Moreover, the residence time of the catalyst in the regenerators is lower too, due to the higher catalyst circulation rate. These temperature evolutions with COR are in agreement with the results presented by Malay et al. (1999). However, no maximum was found in the regenerators' temperature profiles, as presented in the works of Arbel et al. (1995b) and Han and Chung (2001b). Nevertheless, it is important to note that in their works the regeneration system is different from the one presented here.

The effect of COR on VGO conversion and product yields presented in this paper is also in agreement with the results

Table 4
Kinetic data for cracking and combustion reactions used in this study

	Pre-exponential factor	Activation energy (J/mol)
Cracking kinetic parameters		
VGO → LCO	6.59×10^6 (m^3/s/kg)	
VGO → GLN	1.02×10^7 (m^3/s/kg)	
VGO → LPG	2.20×10^6 (m^3/s/kg)	84.2×10^3
VGO → FG	7.35×10^5 (m^3/s/kg)	
VGO → CK	6.36×10^5 (m^3/s/kg)	
LCO → GLN	8.44×10^5 (s^{-1})	77.1×10^3
LCO → CK	7.81×10^5 (s^{-1})	
GLN → LPG	6.95×10^9 (s^{-1})	146×10^3
GLN → FG	2.24×10^9 (s^{-1})	
LPG → FG	1.87×10^{12} (s^{-1})	193×10^3
Deactivation function α	206	
Coke combustion kinetic parameters		
Carbon combustion		
k_{C1}^{dry}	$9.45 \times 10^2 \exp(-1.43 \times 10^5/RT)$ (s^{-1} $Pa^{-0.78}$)	
k_{C1}^{wet}	$2.35 \times 10^4 \exp(-7.92 \times 10^4/RT)$ ($Pa^{0.11}$)	
k_{C2}^{dry}	$7.23 \times 10^1 \exp(-1.59 \times 10^4/RT)$ (s^{-1} Pa^{-1})	
k_{C2}^{wet}	$5.10 \times 10^5 \exp(-1.77 \times 10^4/RT)$ ($Pa^{-0.16}$)	
k_{C3}^{wet}	$1.21 \times 10^3 \exp(-2.71 \times 10^4/RT)$ (s^{-1} $Pa^{-0.1}$)	
$f(X_C)$	$3.0X_C^3 - 2.5X_C^2 + X_C + 0.7$	
Hydrogen combustion: k_3^s	$4.03 \times 10^6 \exp(-1.58 \times 10^5/RT)$ (mol/s/kg cat)	
Heterogeneous CO oxidation: k_4^s	$3.89 \times 10^{-6} \exp(-1.15 \times 10^4/RT)$ (mol/s/kg cat)	
Homogeneous CO oxidation: k_1^g	$8.45 \times 10^{22} \exp(-2.53 \times 10^5/RT)$ (mol/s/m^3)	

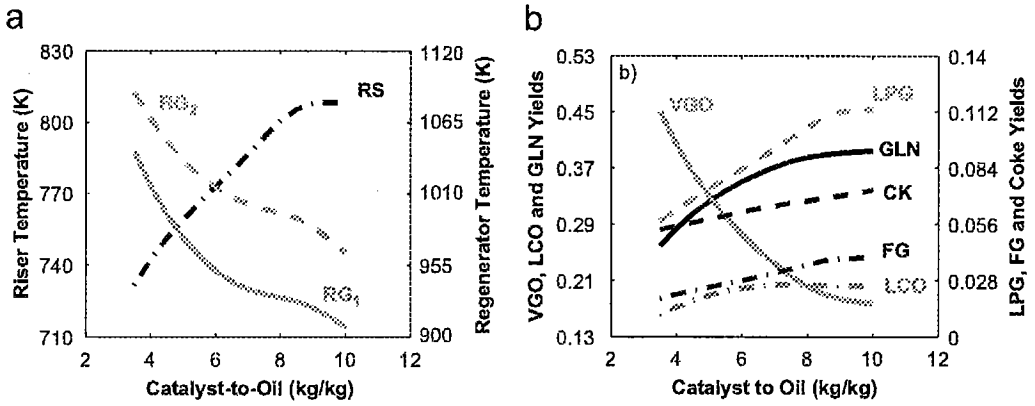

Fig. 3. Effect of COR on temperatures and product yields. (a) Regenerator and riser temperature; (b) VGO and product yields.

presented by Malay et al. (1999). Higher temperatures promote higher conversion rates and, at the same time, a higher COR also means more catalyst, and hence more active centres available for reaction leading again to higher conversions and light product yields.

Fig. 4 shows the profiles of some important process variables along the axial coordinate in the riser. It can be seen that most of the cracking reactions occur in the initial section of the riser. This is an expected result because the highest temperatures and lowest catalyst coke content are encountered at the riser inlet. The velocity profiles (Fig. 4c) clearly show that there is a slip factor between the two phases that decreases along the riser for higher velocities. This slip factor between the two phases is largely due to the formation of clusters of catalyst particles.

In Fig. 4c it can also be observed that both gas and solids velocities increase along the riser due to a molar expansion of about 4 times in the total number of moles in the gas phase. This molar expansion makes the solids void fraction decrease along the riser, while the gas void fraction increases as expected. Fig. 5 shows the dynamic response of the system to a step perturbation in the gas oil feed rate. Decreasing the fresh feed flow rate initially results in a steep increase of the riser temperature (Fig. 5b, RS) due to a higher COR. This immediately leads to a steep increase in conversion (Fig. 5a, VGO). On the other

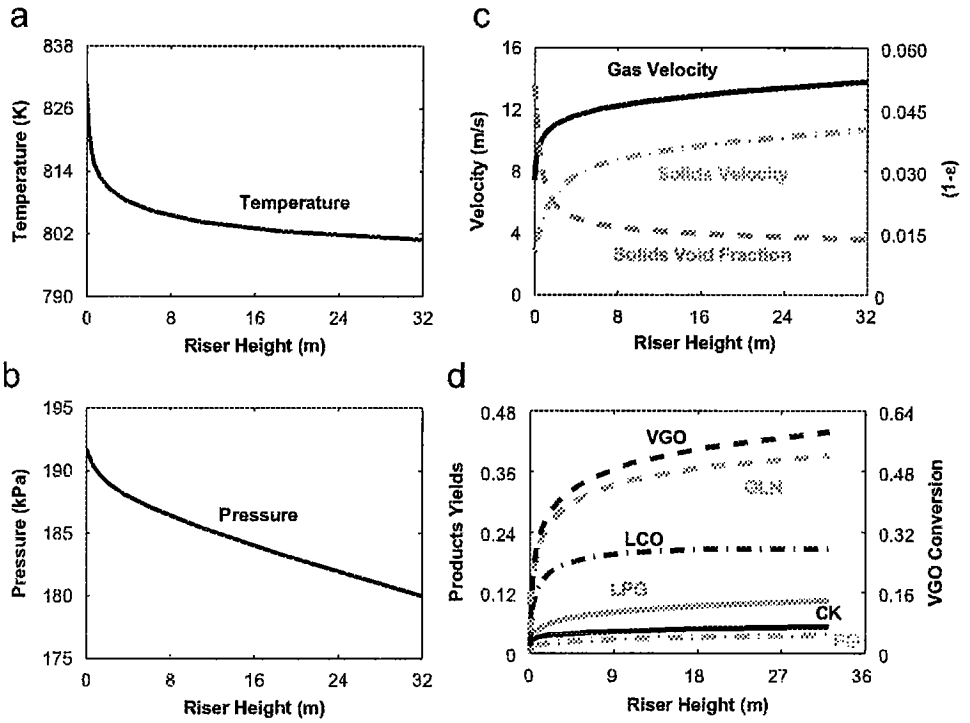

Fig. 4. Steady state profiles along the axial coordinate in the riser. (a) Temperature; (b) pressure; (c) velocity and solids void fraction; (d) product yields and VGO conversion.

hand, a lower concentration of hydrocarbons leads to a pressure decrease in the stripper (Fig. 5c, ST), which causes a steep decrease in the flow rate of spent catalyst and an increase in the regenerated catalyst flow rate (Fig. 5e). The evolution to the new steady state is achieved through a pressure balance compensation caused by a decrease of the catalyst level in regenerator 1 (Fig. 5d, RG1) and an increase of the stripper catalyst level (Fig. 5d, ST). Coke-on-catalyst decreases, due to a lower feed flow rate (Fig. 5e, coke on spent catalyst) and consequently a lower CCR coke contribution. After a small initial increase, the temperature in regenerator 1 also decreases (Fig. 5b, RG1), since the coke content decreased as well as the residence time of catalyst (lower catalyst hold-up). The CO/CO_2 ratio shows an inverse behaviour of the temperature with steeper decreases and increases (Fig. 5f, RG1_CO/CO_2 and RG2_CO/CO_2) after the perturbation occurred. This is expected since the literature shows that σ decreases exponentially with temperature (Vale, 2002). Due to lower temperatures in the regenerators, the temperature in the riser eventually decreases (Fig. 5b, RS_{in}) as well as the VGO conversion (Fig. 5a, VGO). The new steady state shows near the same VGO conversion due to a higher COR, even though the temperatures in the riser and regenerator are lower.

McFarlane et al. (1993) and Han et al. (2001) also present in their papers dynamic simulations in open-loop to feed flow rate perturbations, however real comparisons cannot be done since all the three works present models for different units. It can be seen for example that in our case decreasing the feed flow rate leads to lower temperatures and that riser temperature shows an initial rise caused by the sudden drop in feed flow rate. This is perfectly in agreement with the simulation case presented by McFarlane et al. (1993), on the other hand is in disagreement with the temperatures transient response for the same type of perturbation presented in the work of Han and Chung (2001b), where decreasing the feed flow rate leads to higher temperatures.

The second perturbation sets the fresh feed flow rate back to its initial value. As can be seen, all variables return to their initial steady state.

A perturbation on the air flow rate to regenerator 1 was also made and the dynamic response is presented in Fig. 6. The step decrease of the air flow rate to regenerator 1 initially causes a steep decrease on the temperatures of the regenerators (Fig. 6b, RG1 and RG2), since less air leads to lower coke combustion rates and higher CO/CO_2 ratios (Fig. 6f, RG1_CO/CO_2). The VGO conversion also presents initially a steep increase followed by a steep decrease (Fig. 6a, VGO), since lower coke conversions in the regeneration section lead to higher coke content on the regenerated catalyst at the riser inlet.

Besides decreasing the temperature, a lower quantity of air to regenerator 1 also leads to a lower pressure (Fig. 6c, RG1). This will result in a sudden increase of the catalyst flow rate coming from the stripper (Fig. 6e, spent catalyst), since this flow rate depends on the pressure difference between the bottom of the

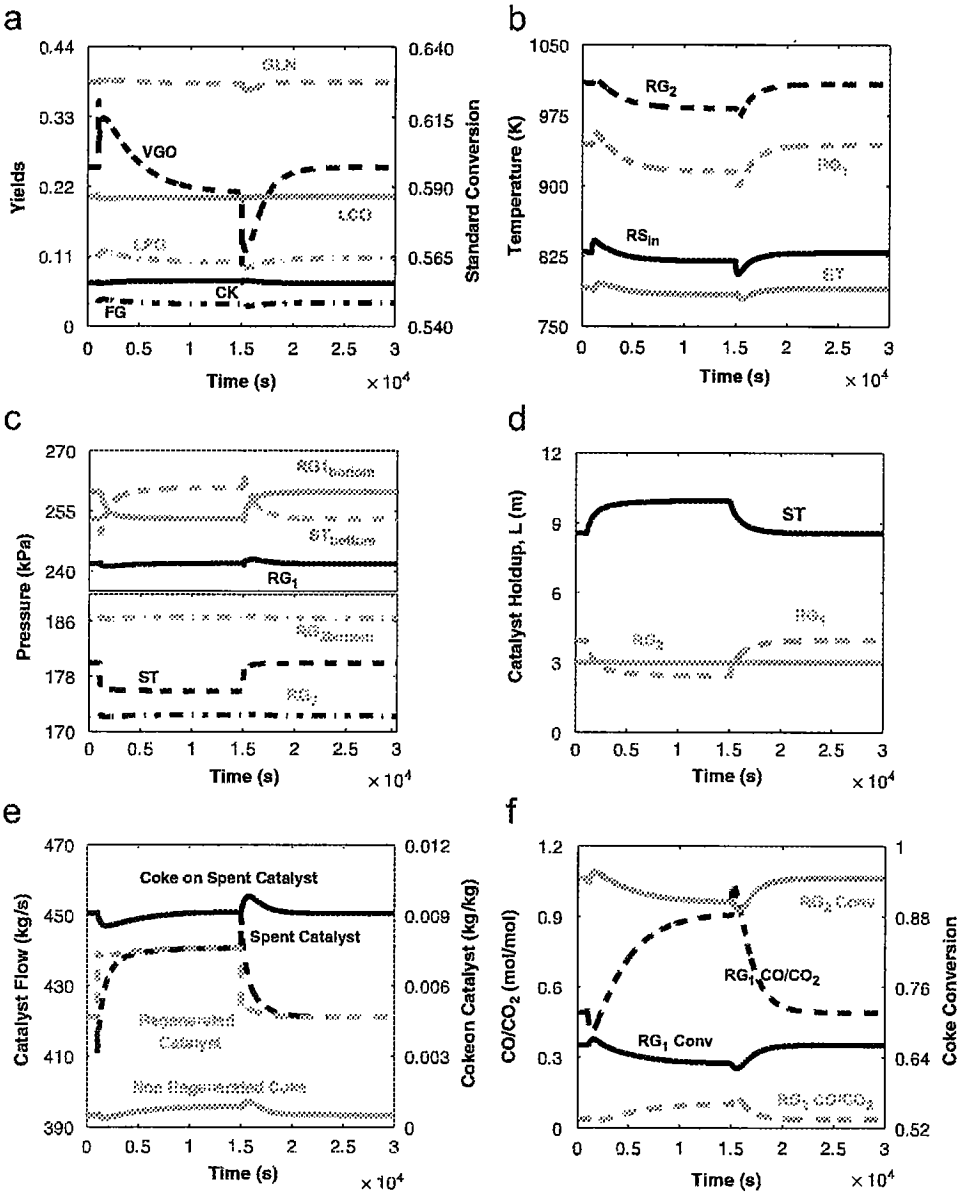

Fig. 5. Open loop dynamic response to a step perturbation of −3% in the fresh feed flow rate at 1000 s, followed by a step perturbation to the initial value of fresh feed flow rate at 15000 s. (a) Product yields and VGO conversion; (b) temperature; (c) pressure; (d) catalyst hold-up; (e) catalyst flow and coke-on-catalyst; (f) ratio CO/CO_2 and coke conversion.

stripper and the pressure of regenerator 1 (see Eq. (22)). The regenerated catalyst flow rate remains practically unchanged (Fig. 6e, regenerated catalyst), since the pressure in the stripper (Fig. 6c, ST) and in regenerator 2 (Fig. 6c, RG2) remain almost constant.

To balance the pressure decrease in regenerator 1 the catalyst hold-up in the stripper will decrease (Fig. 6d, ST), while the bed level in the regenerator 1 will increase (Fig. 6d, RG1). The spent catalyst flow rate then returns to a value slightly higher than its initial one and this will lead to a new steady state where important process variables such as product yields, conversion and temperatures are quite similar to the previous one, before the perturbation had occurred.

Increasing the air flow rate to regenerator 1 to its initial value will lead the system to the initial steady state. However, the dynamic response of the system is not exactly the inverse of the first perturbation in air flow rate at 1000 s, showing smoother increases/decreases in some of the process variables such as temperatures, coke conversion, CO/CO_2 ratio and VGO conversion.

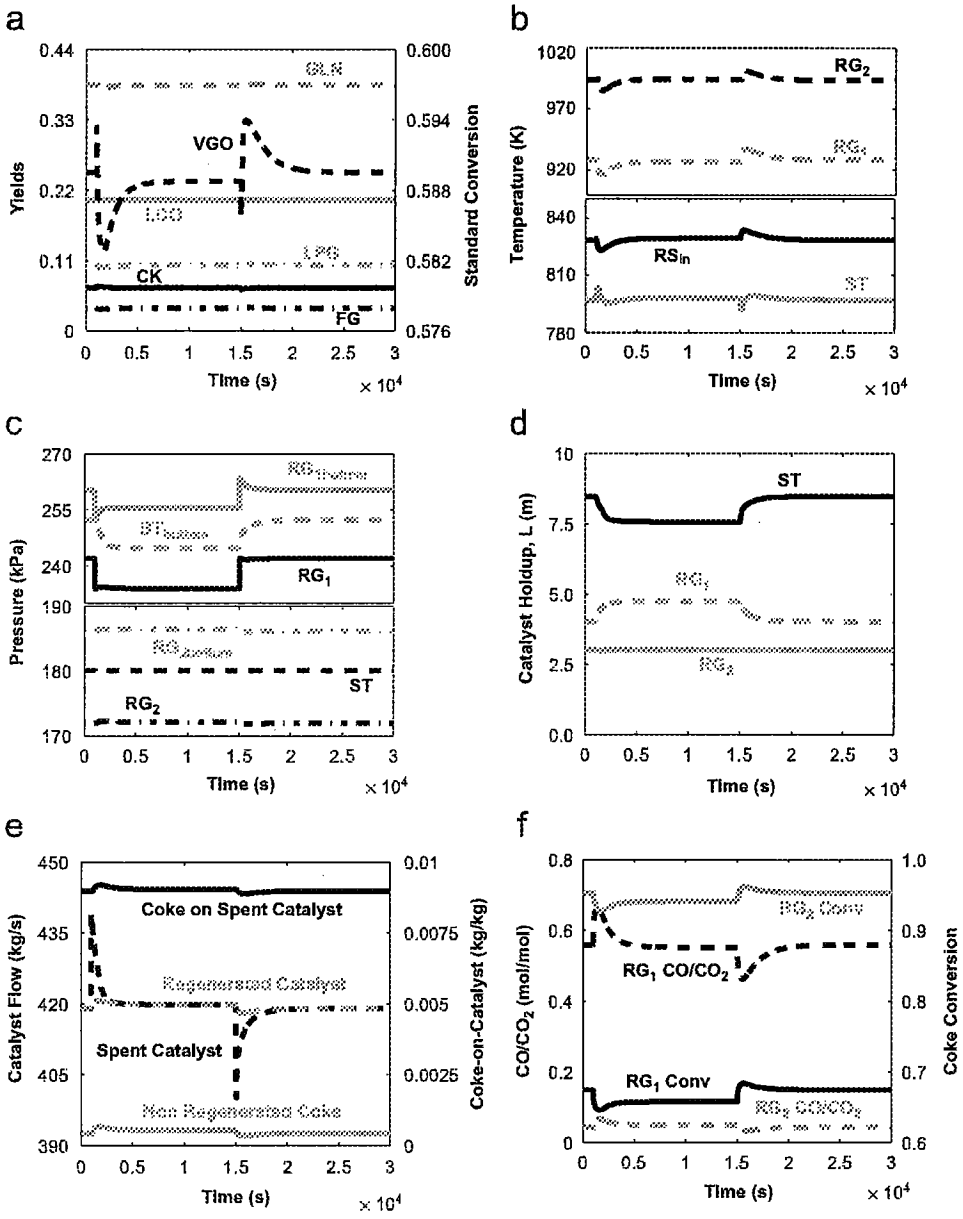

Fig. 6. Open loop dynamic response to a step perturbation of −3% in the air to regenerator 1 flow rate at 1000 s, followed by a step perturbation to the initial value of air to regenerator 1 flow rate at 15 000 s. (a) Product yields and VGO conversion; (b) temperature; (c) pressure; (d) catalyst hold-up; (e) catalyst flow and coke-on-catalyst; (f) ratio CO/CO_2 and coke conversion.

6. Conclusions

A dynamic model has been developed for the simulation of the steady state and dynamic behaviour of a R2R type FCC unit. This model includes a riser reactor, a stripper, a disengager, a two-stage regeneration system and catalyst transport lines.

Studies on FCC units are usually dedicated to traditional FCC unit's designs; however residue cracking units are becoming more important every day due to the increasing need of processing heavier stocks with an economical lower value. This work presents a simulation study on one of this type of units: the R2R FCC unit.

The mathematical model developed allows the prediction of the dynamic behaviour of an industrial R2R unit as well as of its steady state conditions. The open loop study of the dynamics of the R2R unit provides insight into the sensitivity of the response of the main variables in the process to perturbations to the system. From the simulation results, it can be concluded that the model exhibits a behaviour that is consistent with the experimental data and literature results.

An effort was made to assume a compromise between a detailed model with heavy computational needs and a simple model capable of describing the behaviour of the unit. Future work will also include studies of advanced control and real time optimisation based on this model.

Notation

A	Parameter for cluster diameter calculation, dimensionless
A_{ij}	Pre-exponential factor of the reaction lump $i \rightarrow$ lump j, s^{-1} or $m^3/(s\,kg)$
C_i	molar concentration of lump i, mol/m^3
C_p	specific heat capacity, J/(kg K)
C_D	drag coefficient for a particle on an infinite medium, dimensionless
$\hat{C}_i$	mass concentration of lump i, kg/m^3
CCR	Conradson carbon residue in the feed, wt%
CFFE	change of fresh feed enthalpy, Btu/lb
CK	Coke, dimensionless
d	diameter, m
E_{ij}	activation energy of the reaction lump $i \rightarrow$ lump j , J/mol
E_C	energy parameter of the carbon combustion reaction, J/mol
E^g_{aj}	activation energy of the gas reaction j, J/mol
E_{aj}	activation energy of the gas-solid reaction j, J/mol
f	dense-phase fraction, dimensionless
F	mass flow rate, kg/s
FG	Fuel Gas, dimensionless
F_w	gas and solids wall friction force, $kg/(m^2\,s^2)$
$FF°API$	fresh feed°API gravity, dimensionless
FFE	fresh feed enthalpy at riser inlet conditions, Btu/lb
FFK	fresh feed Watson characterization factor (K_w), dimensionless
FFT	fresh feed temperature or combined feed temperature, °F
FFVPE	fresh feed vapor phase enthalpy, Btu/lb
g	gravity acceleration, (m/s^2)
G_c	solidsmass flux, $kg/(m^2\,s)$
GLN	Gasoline, dimensionless
H_k	enthalpy of phase k in stream i, J/kg
k_C	rate coefficient of the carbon combustion reaction,
k^g_j	kinetic rate constant of the gas reaction j, $mols.s^{-1}.m^{-3}$
k^s_j	kinetic rate constant of the gas-solid reaction j, $mols.s^{-1}.kg^{-1}$ cat
k_v	valve flow rating factor, $kg/(s\,kPa^{0.5})$
L	height, m
LCO	Light Cycle Oil, dimensionless
LPG	Liquefied Petroleum Gas, dimensionless
M_w	molar mass, kg/mol
M_2	parameter for cluster diameter calculation, dimensionless
n_{ij}	order of the reaction lump $i \rightarrow$ lump j, dimensionless
N	molar flow rate, mol/s
P	pressure, Pa
Q°_r	global reaction heat at standard conditions, J/s
Q_1	parameter for cluster diameter calculation, dimensionless
$\hat{r}_i$	rate of formation of lump i, $kg/(m^3\,s)$
$\hat{r}_{ij}$	rate of the reaction lump $i \rightarrow$ lump j, $kg/(m^3\,s)$
r^g_j	rate of the gas reaction j, $mol/(m^3\,s)$
r^s_j	rate of the gas–solid reaction j, mol/(kg s)
R	universal gas constant, J/(mol K)
Re	Reynolds number, dimensionless
RxT	reactor temperature, °F
t	time, s
T	temperature, K
u	superficial velocity, m/s
v	velocity, m/s
V	volume, m^3
V_{dry}	partial contribution in dry conditions to carbon combustion reaction rate, mol/(kg s)
V_{wet}	partial contribution in wet conditions to carbon combustion reaction rate, mol/(kg s)
VGO	vacuum gas oil, dimensionless
w^{COR}_{ck}	mass fraction of feed that contributes to cat-to-oil coke, wt%
W	inventory, kg
x_{CCR}	fraction of CCR that converts to coke, dimensionless
x_v	valve opening, $[0-1]$, dimensionless
X_C	carbon conversion of the coke, kg/kg
Y_{ck}	total coke content of catalyst, kg coke/kg catalyst
Y^{cat}_{ck}	catalytic coke content of catalyst, kg catalytic coke/kg catalyst
Y^{CCR}_{ck}	Conradson carbon residue coke content of catalyst, kg CCR coke/kg catalyst
Y_i	component i (in coke) content of catalyst, kg i/kg catalyst
z	axial coordinate, m
Z_g	gas compressibility factor, dimensionless

Greek letters

α	deactivation constant, kg catalyst /kg catalytic coke
γ	parameter for w^{COR}_{ck} calculation, dimensionless
ε	volume fraction, m^3/m^3
ε_{mf}	voidage at incipient fluidization, dimensionless
θ_{SP}	angle of inclination of the standpipe, °
μ_g	dynamic viscosity of the gas, kg/(m s)
ρ	density,kg/m^3
σ	intrinsic CO_2/CO molar ratio, mol/mol

υ	stoichiometric coefficient, dimensionless
ΔH_{crk}	heat of cracking per unit mass of VGO converted, J/kg
Φ	catalyst deactivation function, dimensionless
Ω	cross section, m^2

Subscripts

bed	catalyst bed
bottom	refers to the bottom of an equipment
c	catalyst
ck	coke
cl	cluster
dry	refers to dry conditions in coke combustion
g	gas
i	lump or gaseous species
in	refers to the entrance of an equipment
out	refers to the exit of an equipment
p	catalyst particle
ref	reference
s	steam
wet	refers to wet conditions in coke combustion
MF	main fractionator
RS	riser section
ST	disengager/Stripper section
RG	regenerator section
SP	standpipes section
SP_R	refers to regenerated catalyst standpipe
SP_S	refers to spent catalyst standpipe
1	refers to regenerator 1
2	refers to regenerator 2

Acknowledgements

The author Joana Fernandes thanks the financial support granted by the program POCTI—Formar e Qualificar from Fundação para a Ciência e Tecnologia through the Grant number SFRH/BD/12853/2003.

Appendix

Correlations for the enthalpy change of fresh feed during vaporisation (Montgomery, 1993):

$$\mathrm{FFE} = -13.5 + 0.31\mathrm{FFT}^2 + [0.0025(\mathrm{FF^oAPI} - 10) \times (\mathrm{FFT} - 100)] + [0.04(\mathrm{FFK} - 10)(\mathrm{FFT} - 150)] \quad (68)$$

$$\mathrm{FFVPE} = 135 + 0.29RxT + 0.000161RxT^2 + [1.3(\mathrm{FF^oAPI} - 10)] + [0.075(\mathrm{FFK} - 10)(RxT - 450)] \quad (69)$$

$$\mathrm{CFFE} = \mathrm{FFVPE} - \mathrm{FFE} \quad (70)$$

Correlations for cluster diameter calculation (Xu and Li, 1998; Xu and Kato, 1999)

$$\frac{d_{cl}}{d_p} = \frac{A\rho_p}{\rho_{susp}}, \quad (71)$$

$$A = \frac{(3333u_p g - M_2)(1-\varepsilon_{mf})(\rho_p - \rho_g)}{(Q_1 - 2M_2)\rho_p},$$

$$Q_1 = \frac{(\rho_p - \rho_g)g}{\rho_p}\left[u_g + \frac{u_p\varepsilon_{mf}}{1-\varepsilon_{mf}} + \frac{1}{4}u_t\varepsilon_{mf}^{4.7}\right], \quad (72)$$

$$M_2 = \left(u_{mf} + \frac{u_d\varepsilon_{mf}}{1-\varepsilon_{mf}}\right)g,$$

$$\rho_{susp} = (1-f)(\varepsilon_g - \varepsilon_c)(\rho_p - \rho_g), \quad (73)$$

$$f = \frac{1-\varepsilon}{1-\varepsilon_{mf}}. \quad (74)$$

Correlation for the drag coefficient for a particle on an infinite medium (Rowe and Henwood, 1961):

$$C_D = \begin{cases} \frac{24}{Re_p}(1 + 0.15 \times Re_p^{0.687}) & Re_p < 1000, \\ 0.44 & Re_p \geqslant 1000, \end{cases} \quad (75)$$

$$Re_p = \frac{|v_g - v_c|d_{cl}\rho_g\varepsilon_g}{\mu_g}. \quad (76)$$

Correlation for predicting cat-to-oil coke:

The percentage of feed that contributes to cat-to-oil coke is given by the following correlation:

$$w_{ck}^{COR} = \gamma \cdot \mathrm{COR}, \quad (77)$$

$$\gamma = e^{5.2113 - 0.0144 \times T_{ST}}. \quad (78)$$

The total coke concentration on catalyst in the stripper is then given by

$$Y_{ck,ST} = Y_{ck,RS} + \gamma. \quad (79)$$

References

Ali, H.K.A., Rohani, S., 1997. Dynamic modelling and simulation of a riser type fluid catalytic cracking unit. Chemical Engineering Technology 20 (2), 118–130.

Ancheyta-Juárez, J., López-Isunza, F., Aguilar-Rodríguez, E., 1999. 5-Lump kinetic model for gas oil catalytic cracking. Applied Catalysis A: General 177, 227–235.

Arastoopour, H., Gidaspow, D., 1979. Vertical pneumatic conveying using four hydrodynamic models. Industrial & Engineering Chemistry Fundamentals 18, 123–130.

Arbel, A., Huang, Z., Rinard, I.H., Shinnar, R., 1995a. Dynamic and control of fluidized catalytic crackers. 1. Modeling of the current generation of FCC's. Industrial & Engineering Chemistry Research 34, 1228–1243.

Arbel, A., Rinard, I.H., Shinnar, R., Sapre, A.V., 1995b. Dynamic and control of fluidized catalytic crackers. 2. Multiple steady states and instabilities. Industrial & Engineering Chemistry Research 34, 3014–3026.

Arthur, J.R., 1951. Reactions between carbon and oxygen. Transactions of the Faraday Society 47, 164–178.

Brent, R.P., 1971. An algorithm with guaranteed convergence for finding a zero of a function. The Computer Journal 14, 422–425.

Carabineiro, H., Pinheiro, C.I.C., Lemos, F., Ramôa Ribeiro, F., 2004. Transient microkinetic modelling of n-heptane catalytic cracking over H-USY zeolite. Chemical Engineering Science 59, 1221–1232.

Christensen, G., Apelia, M.E., Hickey, K.J., Jaffe, S.B., 1999. Future directions in modelling the FCC process: an emphasis on product quality. Chemical Engineering Science 54, 2753–2764.

Corella, J., Frances, E., 1991. Analysis of the riser reactor of a fluid cracking unit: model based on kinetics of cracking and deactivation from laboratory tests. In: Occelli, M.L. (Ed.), Fluid Catalytic Cracking–II: Concepts in Catalyst Design. ACS Symposium Series, vol. 452, pp. 165–182.

Daly, C., Tidjani, N., Martin, G., Roesler, J., 2001. Détermination des paramétres cinétiques dans la régénération des catalyseurs de FCC. Technical Report No. 56010, Institut Français du Pétrole.

Das, A.K., Baudrez, E., Marin, G.B., Heynderickx, G.J., 2003. Three-dimensional simulation of a fluid catalytic cracking riser reactor. Industrial & Engineering Chemistry Research 42, 2602–2617.

De Lasa, H.I., Grace, J.R., 1979. The influence of the freeboard region in a fluidized bed catalytic cracking regenerator. A.I.Ch.E. Journal 6 (6), 984–991.

Dean, R.R., Mauleon, J.L., Letzsch, W.S., 1982a. New resid cracker (part 1). Oil Gas Journal 80 (40), 75–80.

Dean, R.R., Mauleon, J.L., Letzsch, W.S., 1982b. New resid cracker (part 2). Oil Gas Journal 80 (41), 168–176.

Elnashaie, S.S.E.H., Mohamed, N.F., Kamal, M., 2004. Simulation and static bifurcation behavior of industrial FCC units. Chemical Engineering Communications 191, 813–831.

Errazu, A.F., De Lasa, H.I., Sarti, F., 1979. A fluidized bed catalytic cracking regenerator model grid effects. The Canadian Journal of Chemical Engineering 57 (April), 191–197.

Faltsi-Saravelou, O., Vasalos, I.A., 1991. FBSim: A model for fluidized bed simulation—II. Simulation of an industrial fluidized catalytic cracking regenerator. Computers & Chemical Engineering 15 (9), 647–656.

Fligner, M., Schipper, P.H., Sapre, A.V., Krambeck, F.J., 1994. Two phase cluster model in riser reactors: impact of radial density distributions on yields. Chemical Engineering Science 49 (24B), 5813–5818.

Gauthier, T., Bayle, J., Leroy, P., 2000. FCC: Fluidization phenomena and technologies. Oil & Gas Science and Technology—Rev. IFP 55 (2), 187–207.

Hagelberg, P., Eilos, I., Hiltunen, J., Lipiäinen, K., Niemi, V.M., Aittamaa, J., Krause, A.O.I., 2002. Kinetics of catalytic cracking with short contact times. Applied Catalysis A: General 223, 73–84.

Han, I.-S., Chung, C.-B., 2001a. Dynamic modelling and simulation of a fluidized catalytic cracking process. Part I: process modeling. Chemical Engineering Science 56, 1951–1971.

Han, I.-S., Chung, C.-B., 2001b. Dynamic modelling and simulation of a fluidized catalytic cracking process. Part II: property estimation and simulation. Chemical Engineering Science 56, 1973–1990.

Hindmarsh, A.C., 1980. LSODE and LSODI. Two initial value ordinary differential equation solvers. ACM-SIGNUM Newslett. 15, 10–11.

Jacob, S., Gross, B., Voltz, S.E., Weekman Jr., V.W., 1976. A lumping and reaction scheme for catalytic cracking. A.I.Ch.E. Journal 22 (4), 701–713.

Kunii, D., Levenspiel, O., 1990. Fluidized reactor models. 1. For bubbling beds of fine, intermediate and large particles 2. For the lean phase: freeboard and fast fluidization. Industrial & Engineering Chemistry Research 29, 1226–1234.

Letzsch, W., Jackson, G., 2004. Residual cracking for the pacific rim. World Refining 24 (6), 42–45.

Li, S., Petzold, L., 1999. Design of new DASPK for sensitivity analysis. Technical Report, Department of Computer Science, University of California Santa Barbara.

Malay, P., Milne, B.J., Rohani, S., 1999. The modified dynamic model of a riser type fluid catalytic cracking unit. The Canadian Journal of Chemical Engineering 77 (February), 169–179.

Marcilly, C.R., Bonifay, R.R., 1996. Catalytic cracking of resid feedstocks. The Arabian Journal for Science and Engineering 21 (4B), 627–651.

McFarlane, R.C., Reineman, R.C., Bartee, J.F., Georgakis, C., 1993. Dynamic simulator for a model IV fluid catalytic cracking unit. Computers Chemical Engineering 17 (3), 275–300.

Montgomery, J.A., 1993. The Grace Davison Guide to Fluid Catalytic Cracking. Part One. W.R. Grace & Co.-Conn.

Morley, K., De Lasa, H.I., 1988. Regeneration of cracking catalyst influence of the homogeneous CO postcombustion reaction. The Canadian Journal of Chemical Engineering 66 (June), 428–432.

Moustafa, T.M., Froment, G.F., 2003. Kinetic modelling of coke formation and deactivation in the catalytic cracking of vacuum gas oil. Industrial & Engineering Chemistry Research 42, 14–25.

Pärssinen, J.H., 2002. Hydrodynamics of low-flux and high-flux circulating fluidized beds. Acta Polytechnica Scandinavica, Mechanical Engineering Series, No. 161, Finnish Academies of Technology, 119pp.

Pinheiro, C.I.C., Lemos, F., Ramôa Ribeiro, F., 1999. Dynamic modelling and network simulation of n-heptane catalytic cracking: influence of kinetic parameters. Chemical Engineering Science 54, 1735–1750.

Pitault, I., Nevicato, D., Forissier, M., Bernard, J.-R., 1994. Kinetic model based on a molecular description for catalytic cracking of vacuum gas oil. Chemical Engineering Science 49, 4249–4262.

Pugsley, T.S., Berruti, F., 1996. A predictive hydrodynamic model or circulating fluidized bed risers. Powder Technology 89, 57–69.

Quann, R.J., Jaffe, S.B., 1992. Structure oriented lumping: describing the chemistry of complex hydrocarbon mixtures. Industrial & Engineering Chemistry Research 31, 2483–2497.

Quann, R.J., Jaffe, S.B., 1996. Building useful models of complex reaction systems in petroleum refining. Chemical Engineering Science 51, 1615–1635.

Radhakrishnan, K., Hindmarsh, A.C., 1993. Description and use of LSODE, the livermore solver for ordinary differential equations. Lawrence Livermore National Laboratory Report, UCRL-ID-113855.

Rowe, P.N., Henwood, G.A., 1961. Drag forces in a hydraulic model of a fluidised bed—part 1. Transactions of the Institution of Chemical Engineers 39, 43–54.

Sabbaghan, H., Sotudeh-Gharebagh, R., Mostoufi, N., 2004. Modelling the acceleration zone in the riser of circulating fluidized beds. Powder Technology 142, 129–135.

Secchi, A.R., Santos, M.G., Neumann, G.A., Trierweiler, J.O., 2001. A dynamic model for a FCC UOP stacked converter unit. Computers & Chemical Engineering 25 (4–6), 851–858.

Takatsuka, T., Sato, S., Morimoto, Y., Hashimoto, H., 1987. A reaction model for fluidized-bed catalytic cracking of residual oil. International Chemical Engineering 27, 107–115.

Vale, H., 2002. Development of a simulator for a complete R2R catalytic cracking unit. Technical Report, Institut Français du Pétrole.

Wang, G., Lin, S., Mo, W., Peng, C., Yang, G., 1986. Kinetics of combustion of carbon and hydrogen in carbonaceous deposits on zeolite-type cracking catalysts. Industrial & Engineering Chemistry Process Design and Development 25 (3), 626–630.

Weekman Jr., V.W., Nace, D.M., 1970. Kinetics of catalytic cracking selectivity in fixed, moving, and fluid bed reactors. A.I.Ch.E. Journal 16 (3), 397–404.

Weisz, P.B., 1966. Combustion of carbonaceous deposits within porous catalyst particles III. The CO_2/CO product ratio. Journal of Catalysis 6, 425–430.

Xu, G., Kato, K., 1999. Hydrodynamic equivalent diameter for clusters in heterogeneous gas-solid flow. Chemical Engineering Science 54, 1837–1847.

Xu, G., Li, J., 1998. Analytical solution of the energy-minimization multi-scale model for gas–solid two-phase flow. Chemical Engineering Science 53, 1349–1366.

Zwinkels, M., Nougier, L., 1997. FCC regenerator simulation model. Technical Report No. 44143, Institut Français du Pétrole.